Charles University, Faculty of Science
Institute of Geochemistry, Mineralogy and Mineral Resources

Study program: Geology
Branch of study: Geology

Bc. Petra Venhauerová

Silver separation technique for isotopic measurement in archaeological samples

Metodologie přípravy vzorků pro měření izotopických poměrů stříbra v archeologických vzorcích

Master`s thesis

Supervisor: RNDr. Jakub Trubač, PhD.
Consultant: Doc., RNDr. Ladislav Strnad, PhD.

Praha 2019

PROHLÁŠENÍ

Prohlašuji, že jsem závěrečnou práci zpracovala samostatně a že jsem uvedla všechny použité informační zdroje a literaturu. Tato práce ani její podstatná část nebyla předložena k získání jiného nebo stejného akademického titulu.

DECLARATION

I declare that I worked the master`s thesis out alone and that I cite all the information sources and literature. This thesis nor her substantial part has not been submitted to obtain another or the same academic degree.

Praha 13. 8. 2019 ….……

ACKNOWLEDGEMENTS

I would like to thank my supervisor, RNDr. Jakub Trubač, PhD. for his expert advice, guidance and encouragement through the whole process.

I would also like to thank Doc., RNDr. Ladislav Strnad, PhD. for his consultations and valuable laboratory instructions, as well as Dr.sc.nat. Tomáš Magna for his comments on the text and technique recommendation with MC-ICP-MS setting. For providing samples of Celtic coins and consultation about the data interpretation, I must thank Mgr. Alžběta Danielisová, PhD. Further, I thank Mgr. Ivana Turková for permission to use a Digital Microscope. I want to thank Marie Fayadová, Lenka Jílková, Ing. Věra Vonásková, and Mgr. Lenka Vondrovicová for their support through my laboratory work and chemical analyses. Advice and comments given by Doc., RNDr. Petr Drahota, PhD., Mgr. Marek Tuhý and MSc Rafael Bieta were a great help in analysing the obtained data.

Finally, I must express my gratitude to my family and friends for their support and encouragement throughout the whole time.

This work was funded from GAČR 13-15390S and OPPK CZ.2.16/3.1.00/21516.

ABSTRACT

Silver isotopes nowadays present a very fast evolving system. One of the field in which this isotopic system is used is archaeology where the silver isotopes are used as a tracer of monetary and power changes between geographical regions. Through statistical analysis of measured data and their comparison with so far published values can be estimated probability of common source area of metal used for coinage.

On Celtic coin samples (180–70 BC) provided by the Institute of Archaeology of the CAS, Prague (A. Danielisová) the isotopic composition of silver was measured. Silver was separated from the matrix elements by a method which uses ascorbic acid to precipitate silver. However, the weights of samples commonly used for this method are generally distinctly higher than the amounts of the obtained fragments of Celtic coins.

Regarding the differences in the method and low weights of fragments, tests with variable concentrations of ascorbic acid and amounts of silver were performed. The amounts of silver used for this method are commonly ~30x-70x higher. The results showed that this method effectively separates silver from matrix elements and is sufficient for higher concentrations of silver; with lower ones the yields are reduced.

The separated silver was measured using MC-ICP-MS. The adjusted instrumental setting for isotopic measurements using MC-ICP-MS proved long-term stability of the measured $^{107}Ag/^{109}Ag$ ratios for NIST SRM 978a.The $\varepsilon^{109}Ag$ values measured by MC-ICP-MS were in agreement with so far published values for historical coins.

Despite the long-standing hypothesis that Celts remelted coins from the Mediterranean area, the statistical tests performed question this hypothesis and do not imply any dependence among the source areas of Mediterranean and Celtic silver, i.e. exploitation of the same deposit type.

Keywords: precipitation, ascorbic acid, silver isotopes, MC-ICP-MS, archaeology

ABSTRAKT

Izotopy stříbra v současné době představují velmi rychle se rozvíjející systém. Jedním z odvětví, které tento izotopický systém využívá je archeologie, kde jsou izotopy používány pro sledování historických změn, především politické moci a oběhu měny mezi geografickými oblastmi. Za použití statistické analýzy naměřených dat a porovnání s doposud publikovanými výsledky, lze odhadnout pravděpodobnost společné zdrojové oblasti kovu použitého na ražbu.

Archeologický ústav AV ČR (A. Danielisová) poskytl vzorky Keltských mincí z oppidálního období (180–70 BC), ve kterých bylo měřeno izotopové složení stříbra. Na separaci stříbra, která je nezbytná pro správné měření izotopových poměrů, byla použita metoda srážení stříbra pomocí kyseliny askorbové. Nicméně navážky stříbra, na které je tato metoda běžně používaná, jsou zpravidla výrazně vyšší než hmotnosti obdržených úlomků Keltských mincí.

Metoda separace stříbra pomocí kyseliny askorbové nebyla zatím na Přírodovědecké fakultě, UK zavedena. Díky spolupráci s Archeologickým ústavem existuje velké množství vzorků pro analýzu, a proto vyvstala otázka, zdali jde zefektivnit separaci a měření izotopů stříbra. Díky této metodě lze přípravu vzorků výrazně zkrátit. Kvůli nízké hmotnosti dostupných vzorků, bylo nutné provést testy s různou koncentrací askorbové kyseliny a použité navážky. Obvyklé navážky, používané pro zvolenou metodu, jsou ~30x-70x vyšší. Výsledky ukázaly, že tato metoda efektivně separuje stříbro od ostatních prvků a je dostačující pro vyšší koncentrace stříbra, s nižšími obsahy se výtěžky snižují.

Následně bylo vyseparované stříbro měřeno na MC-ICP-MS. Stroj vykazoval dlouhodobě stabilitní měření izotopických poměrů $^{107}Ag/^{109}Ag$ pro NIST SRM 978a. Naměřené hodnoty $\varepsilon^{109}Ag$ pomocí MC-ICP-MS jsou v souladu s dosud publikovanými hodnotami získanými pro historické mince.

Navzdory dlouhotrvající hypotéze, že Keltové přetavovali mince pocházející z oblasti Středomoří, provedené statistické testy tuto hypotézu zpochybňují a nenaznačují žádnou závislost mezi společnými zdroji stříbra neboli využíváním stejného typu ložisek.

Klíčová slova: srážení, askorbová kyselina, izotopy stříbra, MC-ICP-MS, archeologie

CONTENT

LIST OF FIGURES

LIST OF TABLES

LIST OF ABBREVIATIONS

AgNPs	Silver Nanoparticles
BC	Before Christ
CCRMP	Canadian Certified Reference Materials Project
CGS	Czech Geological Survey
CRM	Certified Reference Material
DIW	De-ionized Water
DL	Detection limit
FAAS	Flame Atomic Absorption Spectroscopy
IAEA	International Atomic Energy Agency
ICP-MS	Inductively Coupled Plasma Mass Spectrometry
ICP-OES	Inductively Coupled Plasma Optical Emission Spectrometry
JMC	Johnson Matthey Chemicals
MC-ICP-MS	Multicollector Inductively Coupled Plasma Mass Spectrometry
NIST	National Institute of Standards and Technology
ppm	parts per million
SRM	Standard Reference Material

1 INTRODUCTION

The scrutiny of archaeological samples requires an efficient method. Copper (Cu), lead (Pb), and silver (Ag) isotopes are used as a tool for measuring archaeological artefacts (Desaulty et al., 2011; Desaulty and Albarede, 2013; Albarède et al., 2016). Silver is among noble metals, and its discovery is hidden in the ancient past (Boyle, 1968). Silver was mined widely by many cultures and used in areas such as trade as a currency; in religion as tools for worshipping god(s); as decoration of objects and buildings; as jewellery; or as kitchen utensils such as cups, bowls or plates.

In the last years, the interest in silver isotopes has increased. They are used to analyse meteorites (Kelly and Wasserburg, 1978; Kaiser and Wasserburg, 1983; Chen and Wasserburg, 1996; Carlson and Hauri, 2001; Woodland et al., 2005; Schönbächler et al., 2008), geological samples (Schönbächler et al., 2007; Chugaev and Chernyshev, 2012; Mathur et al., 2018; Argapadmi et al., 2018), environmental samples (Luo et al., 2010), commercial products (Yang et al., 2009) or archaeological findings (Desaulty et al., 2011; Desaulty and Albarede, 2013; Albarède et al., 2016). To sum up, Ag isotopes can be used for exploring noble metal deposits, tracking environmental processes, labelling nanoparticles or tracing monetary changes through history.

The method adopted for separating silver from archaeological samples has not so far been tested and established at our faculty. Therefore the methodology required is optimised, fast, cheap, and effective for these sample types. The aim of this thesis is to apply recent findings, in the field of analytical, and instrumental bias improvements for MC-ICP-MS, to the archaeological field. The separation method is based on the work of Stathis (1948), Desaulty et al. (2011), and Albarède et al. (2016); and is adjusted for present laboratory settings. The instrumental bias improvements for measuring on MC-ICP-MS are based on papers by (Woodland et al., 2005; Baxter et al., 2006; Schönbächler et al., 2007; Guo et al., 2017).

Also noted is an overview of variation, fractionation and application of Ag isotopes. Next follows a summary of the different types of separation methods adapted for specific samples and their recovery rates. A summary of data processing approaches and corrections due to instrumental mass discrimination (fractionation), spectral interferences and matrix effect are last.

The method which was tested and then used for receiving isotopic composition of Celtic coins from 1^{st}-2^{nd} century BC from two areas in the Czech Republic is described (Chapter 5.4.2). Both areas are historical oppida (Gallic tribe, Boii); the first, Stradonice, is located in Bohemia and the second one, Stare Hradisko, is situated in Moravia.

2 STATE OF KNOWLEDGE

Stable isotope systems are conventionally divided into two groups: traditional: carbon (C), oxygen (O), hydrogen (H), nitrogen (N) and sulphur (S); and non-traditional: such as lithium (Li), magnesium (Mg), silicon (Si), zinc (Zn) copper (Cu), molybdenum (Mo) and many others (Johnson et al., 2004; Teng et al., 2017).

Non-traditional stable isotopic geochemistry is a relatively new field of interest. The beginnings of silver isotopes measurements can be followed back to Hess et al. (1957). They suggested that the silver isotopic content in meteorites may be used to expose solar system history; however, they pointed out it is unlikely. This suggestion was confirmed two decades later by measurements on volatile-depleted meteorites (Pd-Ag system, Chapter 3.1), characterised by extremely high ratios of Pd/Ag, where the disparity between Ag and Pd is sufficiently significant for the usage of TIMS (Kelly and Wasserburg, 1978; Kaiser and Wasserburg, 1983). The multi-collector inductively coupled plasma mass spectrometry (MC-ICP-MS) was used for scientific purposes for the first time in the early `90s (Walder and Freedman, 1992) and assuaged notoriously known issues from TIMS concerning large analytical uncertainties and large sample amounts often required for high-precision data. The development held more extensive usage of MC-ICP-MS back for nearly two decades. MC-ICP-MS allowed, with link to the higher precision of the instrument, focus on lower disparities in ratios of measured samples. It was only then that the Pd-Ag system with medium or low Pd/Ag ratios or terrestrial processes were possible to study.

Silver has 38 discovered isotopes so far with masses from 93 up to 130, and more are predicted to be uncovered in the future (Schuh et al., 2010). These artificial, non-stable silver isotopes have half-lives from a couple of days to milliseconds. Silver has two, naturally occurring stable isotopes, ^{107}Ag with an exact atomic weight of 106.905 095, and ^{109}Ag of mass 108.904 754 (5) (Peiser et al., 1984). The abundance of the ^{107}Ag is slightly higher: 0.518 392 (6), than the one of ^{109}Ag: 0.481 608 (Meija et al., 2016). These mentioned values have been measured on “normal material” which is defined below.

> *“The material is a reasonably possible source for this element or its compounds in commerce, for industry or science; the material is not itself studied for some extraordinary anomaly and its isotopic composition has not been modified significantly in a geologically brief period.”*
>
> *(Peiser et al., 1984)*

The standard reference material for silver is NIST SRM 978a, created by Powell et al. (1981) from SRM 748, silver metal with high purity; and certified by the National Bureau of Standards three years later as an isotopic standard (Rasberry, 1984).

Isotopic data are expressed relative to the above mentioned SRM 978a in either $\varepsilon^{107}Ag$, $\varepsilon^{109}Ag$ or $\delta^{109}Ag$ values (Equation 1-3).

$$\delta^{109}Ag = \left(\frac{\left(^{109}Ag/^{107}Ag\right)_{sample}}{\left(^{109}Ag/^{107}Ag\right)_{standard}} - 1\right) \times 1000 \quad (1)$$

$$\varepsilon^{109}Ag = \left(\frac{\left(^{109}Ag/^{107}Ag\right)_{sample}}{\left(^{109}Ag/^{107}Ag\right)_{standard}} - 1\right) \times 10{,}000 \quad (2)$$

$$\varepsilon^{107}Ag = \left(\frac{\left(^{107}Ag/^{109}Ag\right)_{sample}}{\left(^{107}Ag/^{109}Ag\right)_{standard}} - 1\right) \times 10{,}000 \quad (3)$$

There exist several silver standard materials which are used for measuring Ag isotopic composition in unique types of samples, such as standard materials for nanosilver, environmental specimens or precious metals (Luo et al., 2010; Murray, 2010; NIST, 2015). Reference materials used for tracking environmental processes are; industrial sludge (SRM 2781), sediments (CRM PACS-2), domestic sludge (SRM 2782) or fish liver (CRM DOLT-4); compared in Luo et al. (2010). Among geological standards are IAEA-S-1, IAEA-S-2 and IAEA-S-3, they are silver sulphides used as isotopic Reference Materials for sulphur. Except for IAEA-S-2, which was synthesised out of gypsum evaporated from seawater, the resource material of the IAEA-S-1 and IAEA-S-3 was sphalerite (IAEA, 2009). The measured isotopic composition of these above-mentioned reference materials is listed in Table 1.

Table 1. The isotopic composition of silver in reference materials for environmental samples and isotopic reference materials for sulphur (Luo et al., 2010; Guo et al., 2017).

Reference Material	Description	δ^{109}Ag (2SD, n = 4)
SRM 2781	industrial sludge	–0.044 ± 0.014
CRM PACS-2	sediment	+0.025 ± 0.014
SRM 2782	domestic sludge	+0.061 ± 0.010
CRM DOLT-4	dogfish liver	+0.284 ± 0.014
IAEA-S1	Silver Sulphide	+0.020 ± 0.011
IAEA-S2	Silver Sulphide	–0.029 ± 0.005
IAEA-S3	Silver Sulphide	–0.027 ± 0.006

In further listed subchapters findings of silver isotopes' fractionation, its variations throughout materials, possible applications, e.g. deposit geology, environmental sciences and finally archaeology are adduced.

2.1 Variations and fractionation of silver isotopes in nature

As summarised by Schauble (2004), the different atomic weights of isotopes of one system lead to differential behaviour in most processes. For example, the heavier isotope of a system creates stiffer bonds; in contrast, reactions of heavier species are slowlier. The stiffer bonds tend to correlate with the higher oxidation state, covalent bonds and low coordination number.

This different behaviour of the isotopes of an element leads to fractionation of its isotopes based on their relative mass difference; that can be further sorted according to the nature of the processes into chemical, physical and biological. Fractionation during biological processes is generally due to the propensity of elements to bind to organic particles. Physical fractionation is caused by external conditions such as temperature or evaporation, whereas the chemical fractionation is influenced by reactions of elements with its surrounding and depends, among others, on the type of a bond or equilibrium versus kinetic processes.

Basic silver characterisation is listed in Table 2.

Table 2. Silver characterisation (Heslop and Jones, 1982; Kramida et al., 2018).

Silver properties	Values
Atomic number	47
Electron configuration	[Kr] $4d^{10}$ $5s^{1}$
Oxidation states	1, 2, (3)
Ionization energies (eV)	1^{st} 7.5762 2^{nd} 21.49 3^{rd} 34.83

Silver fractionates during biological (Luo et al., 2010), chemical, e.g. redox reactions (Mathur et al., 2018), and also physical processes such as precipitation of Ag in the presence of Cl^- (Luo et al., 2012).

Experiments performed by Luo et al. (2012) disclosed how the loss of Ag during precipitation, induced by Cl^-, influences the isotopic composition (Figure 1). Chloride is naturally present in water reservoirs and for precipitation of Ag are necessary relatively low amounts; as a result, natural precipitation of Ag can be expected which would lead to the enrichment of the sediment with a lighter isotope. Their experiments showed that the Ag isotope fractionation is significant; the precipitation of Ag resulted in enrichment of the precipitate in the lighter isotope while the heavier one stayed in the remaining solution.

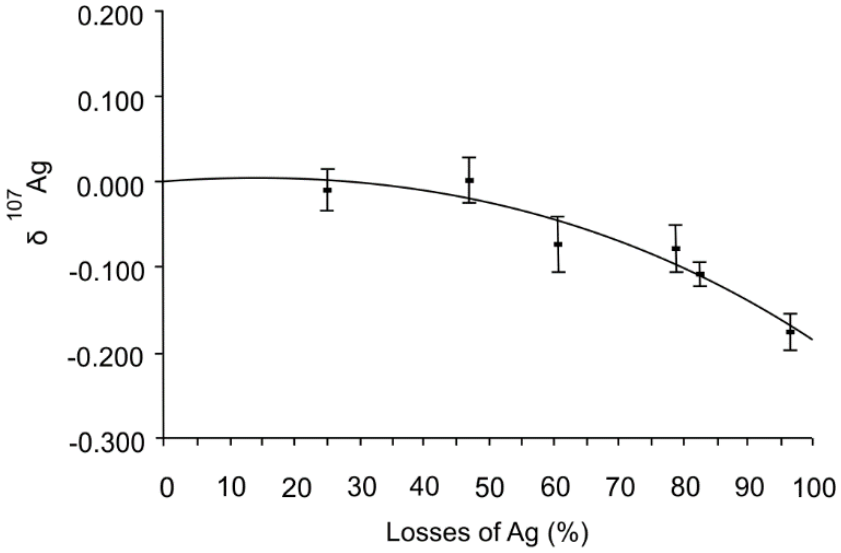

Figure 1. Effect of Cl^- on the isotopic composition of Ag (according to Luo et al. (2012)).

Sturgeon et al. (2006) investigated the volatilisation of Ag caused by the UV photolysis; the Ag can thus be transferred from water into the atmosphere. Luo et al. (2012) suggested that this process can lead to measurable isotope effects. However, the experiments did not show any significant fractionation as a consequence of photo-volatilisation. Fujii and Albarede (2018) pointed out fractionation due to the type of compound that binds with Ag. They concluded the dependence of Ag isotope fractionation on the bond length, coordination numbers of the compound and temperature.

For those reasons, variations in isotopic composition among different type of samples and environments exist; variations in some sample types (e.g. ore deposits) are more significant than in other (e.g. silver coins) (Figure 2). For example, the variation of ε values of Ag among one deposit type is more significant than predicted (Mathur et al., 2018; Argapadmi et al., 2018), i.e. the variability of ε values expected on a global scale can be found among one deposit.

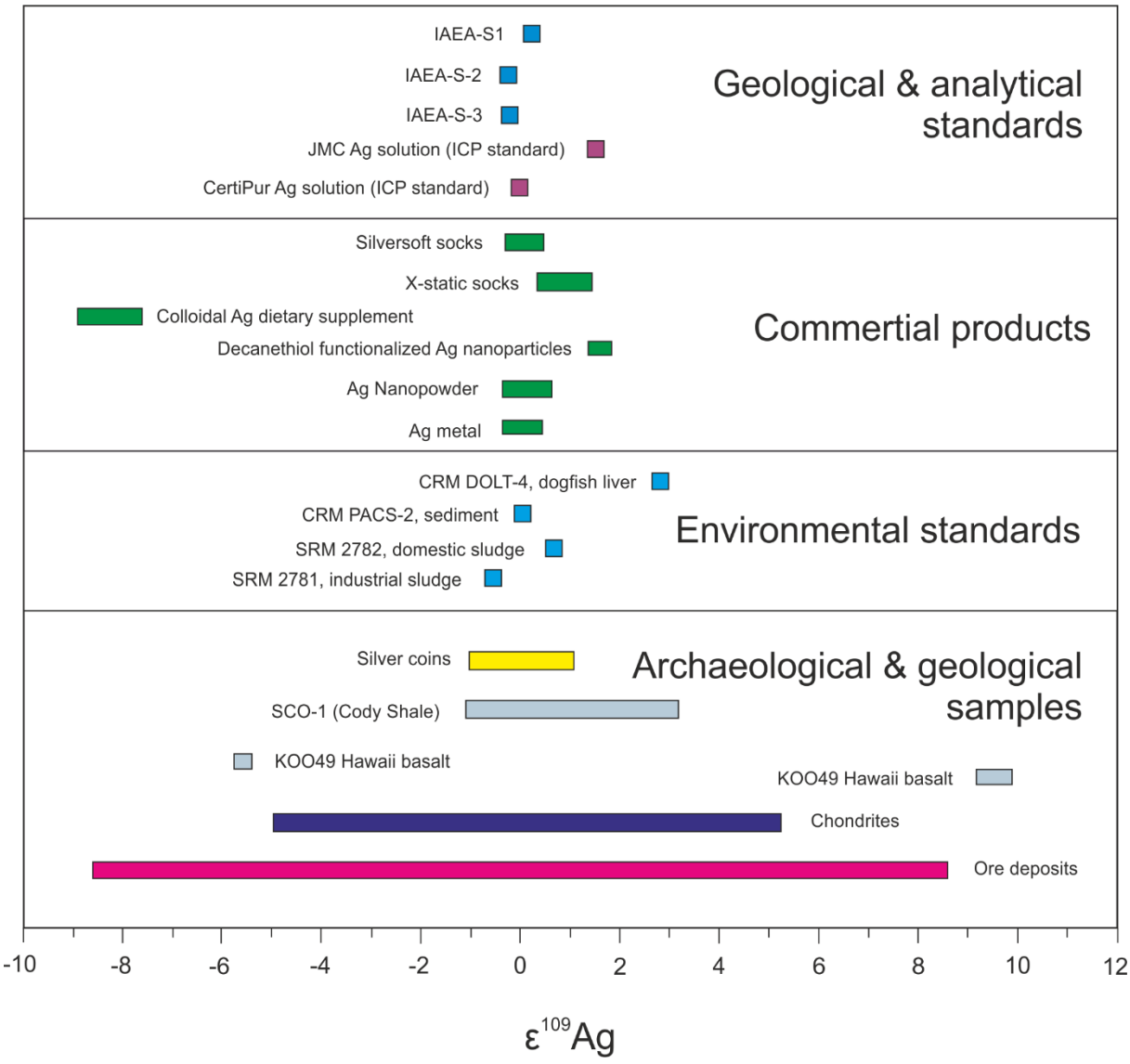

Figure 2. Variation of ε^{107}A in a wide variety of samples (according to Guo et al. (2017)).

3 APPLICATION OF SILVER ISOTOPES

The isotope ratios are usually not used directly. The variations in isotopic compositions are minimal so for an easier comparison values of ε^{107}Ag, ε^{109}Ag for mostly geochronological and geological applications are used (Holland et al., 2001; Woodland et al., 2005; Schönbächler et al., 2007; Schönbächler et al., 2008; Argapadmi et al., 2018) or lately even for geological specimens appears more frequently values of δ^{109}Ag (Yang et al., 2009; Luo et al., 2010; Luo et al., 2012; Lu et al., 2016; Guo et al., 2017; Mathur et al., 2018).

3.1 Cosmochemistry

One of the possible application of silver isotopes is in cosmochemistry (Kelly and Wasserburg, 1978; Kaiser and Wasserburg, 1983; Chen and Wasserburg, 1996; Carlson and Hauri, 2001; Woodland et al., 2005; Schönbächler et al., 2008).

Silver is part of the extinct ^{107}Pd–^{107}Ag chronometer; in the early Solar System, ^{107}Pd decayed to ^{107}Ag with a half-life of 6.5 Myr. The Pd-Ag chronometer is used to estimate the timing of planetesimals formation. Kaiser and Wasserburg (1983) state that the changes in the isotopic composition imply high solar activity during the creation of planetesimals. Carlson and Hauri (2001) mentioned the possible use of this chronometer to survey dynamics and evolution of the Earth`s core and mantle. Schönbächler et al. (2008) studied depletion caused by the volatility of the elements. However, (Fujii and Albarede, 2018) argued that Ag isotopes are suitable for geochronological purposes due to a substantial low-temperature fractionation.

3.2 Geology

Silver isotope geochemistry has several applications in the field of exploration/economic geology, the genesis of ore deposit forming processes (e.g. tracer of source and transportation systems for gold) and conceivably hydrometallurgical processes (Mathur et al., 2018; Argapadmi et al., 2018).

Irisawa and Hirata (2006) investigated the isotopic fractionation of tungsten (W) reference materials and summarised the major cause of natural isotopic variations of W to be caused by reactivity during redox reactions, condensation or evaporation. The fractionation due to changes during the chemical reactions can also be applied to Ag. Mathur et al. (2018) presented a new set of data which doubled the available ones for silver and ore deposits. The most distinct value obtained for native supergene Ag in the mesothermal deposit is δ^{109}Ag = 2.1; the most other values range between –0.86 and +0.8 ‰. Mathur et al. (2018) emphasised no apparent correlation between the type of the deposits or locality and explained isotopic variations by the changes of Ag oxidation state in redox reactions, adsorption reactions and precipitation onto minerals (performed tests with MnO_2 and FeOOH).

A recently published article by Argapadmi et al. (2018) focuses on the possible usage of silver isotopes as a tracer of the gold deposits forming processes. Argapadmi et al. (2018) observed the variability in gold samples from two distinct localities from the Barberton Greenstone Belt in South Africa; the values of δ^{109}Ag were ranging from –0.42 ± 0.04 to 0.36 ± 0.04. Whereas the two sites originated from the common primary deep reservoir, they differ significantly in the Ag isotopic composition; the first mine showed positive δ^{109}Ag values, whereas the second was marked by negative δ^{109}Ag values. Argapadmi et al. (2018) demonstrate this difference by changes in the redox states where the oxidised form ($Ag^{+}_{(aq)}$), compared with the reduced ($Ag^{0}_{(s)}$), is depleted in the lighter isotope, and by fractionation processes

during the genesis of the rock formation. Collectively, Ag closer to the source appears to be enriched in the ^{107}Ag, whereas in the more remote parts it is enriched in ^{109}Ag.

Argapadmi et al. (2018) also suggest a possible temperature dependence of the fractionation, even though Mathur et al. (2018) do not mention any temperature-dependent fractionation. Therefore, for calculations of the fractionation factor, Argapadmi et al. (2018) neglected the effect of temperature and assumed mass-dependence (Equation 4).

$$10^4 ln\alpha^{109}Ag = \varepsilon^{109}Ag\left(Ag^{+}_{(aq)}\right) - \varepsilon^{109}Ag\left(Ag^{0}_{(metal)}\right) \qquad (4)$$

The fractionation factor calculated for Ag is 6 for the ε^{109} values; i.e. 0.6 for the δ^{109} values.

3.3 Nanoparticles

Silver nanoparticles (AgNPs) are widely used due to the antimicrobial effect. Beside that AgNPs are used in mass cytometry; resulting in usage for immunology and biomarker exploration (Schulz et al., 2017).

Silver nanoparticles are added into a wide variety of commercially used products such as plastic containers, bags, fridges, clothes (e.g. socks), bandages, food supplements, water filters and many more. Owing to that, it has become essential to monitor what effect AgNPs bring to human health since Ag has strong antimicrobial effects and little sizes of NPs (1 to 100 nm) leads to special behaviour and characteristics compared to the larger particle sizes of Ag.

Beer et al. (2012) stressed the toxicity of AgNPs based on the present proportion of silver ion in the suspension. They stated that the presence of Ag ions in AgNPs has a substantial part in the toxic effect of AgNPs in suspension and argued that routine measurements and reports on the volume of silver ions in AgNPs should be implemented.

Another possible application of AgNPs can be to use isotopically labelled AgNPs for tracking environmental processes or source material. Junk et al. (2016) emphasised that the detection limits for tracking ^{107}Ag-enriched materials are surprisingly low; it is possible to detect enrichments of ^{107}Ag up to 0.26 ‰ of the normal Ag background. Lu et al. (2016) argued that further investigation is needed to unequivocally prove if the isotopic composition can specify the source of AgNPs due to the fact that natural AgNPs indicated the reverse direction of isotope fractionation in relation to artificial AgNPs in solution.

3.4 Environmental applications

Silver is characterised by the Environment Canada Chemical Management Plan (CPM) as a high priority toxic metal. Luo et al. (2010) emphasised the usage of Ag isotope fractionation, induced by chemical

and biological processes, as a fingerprinting source of the Ag in the cycle. Moreover, silver could serve as a delicate forensic tool.

Results of the isotopic composition of several environmental standards (SRM 2781, CRM PACS-2, SRM 2782 and CRM DOLT-4) by Luo et al. 2010) are listed in Table 1. Significantly different isotopic composition of the fish liver, DOLT-4, may be explained by fractionation reflecting biological processes. Similarly, δ^{109}Ag values of SRM 2781 (industrial sludge) can imply enrichment of ^{107}Ag from the anthropogenic source.

Luo et al. (2012) conducted an experiment to monitor possible physical fractionation occurring during incorporation of Ag from the habitat (i.e. water reservoir, lake) into the sediment. The experiments were done using CRM PACS-2 (sediment) and Ag food supplement with anomalous isotopic composition of $\delta^{109}Ag = -0.83 \pm 0.03$ (1SD, n = 4). The experimentally obtained values corresponded with theoretically calculated values from a mixing model with two end members. To sum up, Ag can be possibly applied for tracking the Ag source throughout the earth´s system.

3.5 Archaeology

Silver, among other stable isotope systems such as copper and lead, was used as a means for monitoring historical power changes between geographical regions by monitoring the isotopic composition of silver coins (Bendall et al., 2009; Desaulty et al., 2011; Albarède et al., 2012; Desaulty and Albarede, 2013; Albarède et al., 2016).

Among new applications in the field of archaeology is the measurement of Ag isotope compositions in samples containing low concentrations of Ag (between 5 mg/g and 123 mg/g) (Brügmann et al., 2019). Brügmann et al. (2019) monitored changes in the Ag isotopic ratios in the gold nuggets. They reported variation of δ^{109}Ag between –0.58 and 0.83; however, they pointed out homogenity of the nugget interior and suggested fractionation due to loss of Ag toward the edge of the grain.

Desaulty et al. (2011) used Ag isotopes for tracking changes in the composition of Spanish silver coins from the 16th to 18th century. The most important longstanding theory was that the new influx of precious metals from new American colonies of the Spanish empire could cause massive inflation in the 16th-17th century in Spain. According to the measured values, the isotopic change in coins does not overlap with the period of inflation. Desaulty and Albarede (2013) set their research on the same period of time in the area of early Stuart Europe and aimed to comprehend ways through which American gold was exported. The analysis showed that dominated coinage metal to this area came from Mexico and Europe. Therefore, these authors focused on deciphering where silver from Spanish America's mines ended up. Confirmed was the existence of the two mostly disconnected paths: The Potosi–China route and The Mexico–Europe routes. As an explanation, Desaulty and Albarede (2013) suggest the geographical

position of the mines; Potosi mine lies on the west coast of South America and the transport of the silver through the area of today's Brazil would be complicated.

Albarède et al. (2016) used stable isotope compositions of silver to track the cash flow during the Second Punic War. Coins from the periods after and before the monetary reform in 211 BC were measured, during which the weight of silver coins was radically reduced, as a means to stop the inflation. The pre-reform metal comes from Spain and probably was delivered into Rome as a war penalty after the First Punic War from Cartago. Post-reform silver is isotopically different and probably came from plundering the south part of Apennine (Capua) and Syracuse.

Fujii and Albarede (2018) presented two types of statistical tests (Mann-Whitney U-test and t-test) according to which it is possible to say if the analysed coins were produced from metal originating from similar provinces or if they were coined from Ag originating from distinct ores.

The comparison of ε^{109}Ag variability in silver coins, based on their geographical position and era of origin, is presented in Figure 3. Generally, the results plot mostly in the range of 0 ± 1 ε^{109}Ag.

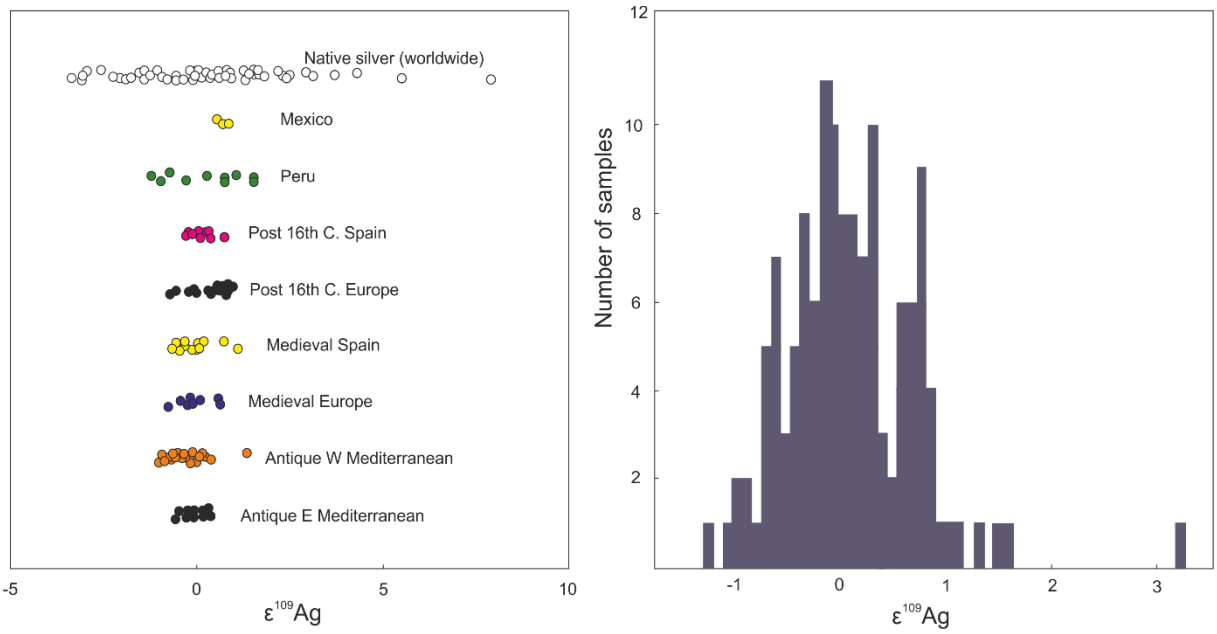

Figure 3. Distribution of so far published ε^{109}A values of historical coins. On the left are published values of ε^{109}Ag in silver coins and reported variations in deposits. The histogram presents density of reported values; the major amount of samples is clustered around 0, another significant peak is around ε^{109}Ag of +0.8 indicating possible low-temperature origin (according to Fujii and Albarede (2018)).

4 HISTORY OF THE SILVER ISOTOPE MEASUREMENTS

A major part of the samples used for the Ag isotope analysis is multi-elemental. Therefore, the desired element, silver in this case, must be separated to circumvent matrix effects during analysis on MC-ICP-MS. The separation methods attempted to secure high Ag recovery. The importance of obtaining complete yields due to excessive fractionation during the separation by column chromatography was demonstrated by Schönbächler et al. (2007). They noticed that in one out of three replicates the observed ε values were distinct from the other two; namely, the result differed by 1.1 ε from the average value of the other two replicates. The first sample yielded 70 % of the original Ag because of a shift in the elution peak. Therefore, Schönbächler et al. (2007) ran an experiment based on collecting the first 70 % of Ag eluted separately and followed by the remaining 30 % of Ag. The measured ε^{107}Ag values proved significant fractionation; first 70 % had ε^{107}Ag = 0.96 whereas the lately eluted residuum had ε^{107}Ag = –4.11.

History of methods used for Ag separation goes back to the first analysis of Ag isotopes used for Pd-Ag system, i.e. ^{107}Pd-^{107}Ag chronometer (Kelly and Wasserburg, 1978; Kaiser and Wasserburg, 1983; Chen and Wasserburg, 1996; Carlson and Hauri, 2001). Previously, the analysis was performed using TIMS technique (Kelly and Wasserburg, 1978; Kaiser and Wasserburg, 1983). More recently, Carlson and Hauri (2001) presented a new high-precision MC-ICP-MS technique for measuring silver isotopes, which enabled them to focus on the meteorites with low Pd/Ag ratios (also Woodland et al., 2005).

4.1 Matrix elements

The separation by column chromatography is not 100 % efficient to remove all matrix elements, especially when they are present in significantly higher quantities than Ag. Therefore, knowledge of how matrix elements influence the measurement and how appreciably is necessary; as well as efficient ways how to correct these impacts.

4.1.1 Matrix effect and spectral interferences

Matrix elements remaining in the solution even after silver ion-exchange separation are a source of matrix effects due to the formation of isobaric and polyatomic interferences which contribute to the inaccuracy of the measurements. Among these matrix elements, titanium (Ti) and iron (Fe) (causing matrix effect when presented in higher concentrations) are the most important; further, copper (Cu), zinc (Zn), niobium (Nb), rubidium (Rb), gallium (Ga), gadolinium (Gd), germanium (Ge), strontium (Sr), yttrium (Y), zirconium (Zr), cadmium (Cd), molybdenum (Mo) noted by Schönbächler et al. (2007). Isobaric interferences are caused by another element having isotopes of the same mass as the element of interest. In case of silver, there are no elements creating isobaric interferences; although since Pd is added to the samples for the correction of mass bias, it needs to be taken under consideration also

elements forming isobaric interferences with specific Pd masses. Subsequently, polyatomic interferences are caused by atoms or molecules formed from matrix element with itself – dimer, or with argon (Ar), oxygen (O), nitrogen (N), or carbon (C); these interferences are formed during sample ionisation in the plasma. Such formed compounds can interfere with masses of Ag, Pd or both. Possible interferences on Pd and Ag masses are stated in Table 3.

Table 3. Possible polyatomic and isobaric interferences on masses of Pd and Ag for MC-ICP-MS.

	^{104}Pd	^{105}Pd	^{106}Pd	^{107}Ag	^{108}Pd	^{109}Ag
Isobaric interferences	$^{208}Pb^{2+}$ *		$^{106}Cd^{+}$		$^{108}Cd^{+}$	
Polyatomic interferences	$^{88}Sr^{16}O^{+}$	$^{65}Cu^{40}Ar^{+}$ $^{89}Y^{16}O^{+}$	$^{66}Zn^{40}Ar^{+}$ $^{90}Zr^{16}O^{+}$	$^{67}Zn^{40}Ar^{+}$ $^{71}Ga^{36}Ar^{+}$ $^{91}Zn^{16}O^{+}$	$^{68}Zn^{40}Ar^{+}$ $^{92}Mo^{16}O^{+}$	$^{69}Ga^{40}Ar^{+}$ $^{73}Ge^{36}Ar^{+}$ $^{93}Nb^{16}O^{+}$

* double charged

4.1.2 Historical smelting process

The samples of interest in this thesis are coins which undergo the smelting process during the separation of Ag from ores (silver-bearing minerals), and coinage process. These processes lead to a reduction in concentration or elimination of some of the possible matrix elements.

It is not easy to track the historical smelting processes of ores; nevertheless, several papers summarised old historical sources (Vaněk and Velebil, 2007; Pernicka, 2014). The following description of the historical metallurgical process results from the description given by Vaněk and Velebil (2007). The first steps include sorting, milling and floating of the ore material. The second step is roasting, during which the sulfides are transferred into oxides (Equation 5 and 6; X = metal element). Most of the S, arsenic (As), antimony (Sb), and selenium (Se) leaves the ore and enters the smoke in the form of oxides.

$$2\,XS + 3\,O_2 \rightarrow 2\,XO + 2\,SO_2 \quad (5)$$

$$XS + 2\,O_2 \rightarrow XSO_4 \quad (6)$$

The third step was reduction smelting (Equation 7–12).

$$XS + C \rightarrow CO + X \quad (7)$$

$$XO + Pb \rightarrow PbO + X \quad (8)$$

$$PbO + C \rightarrow Pb + CO \quad (9)$$

$$XSO_4 + 4\,C \rightarrow XS + 4\,CO \quad (10)$$

$$2\,XO + XS \rightarrow 3\,X + SO_2 \quad (11)$$

$$2\,PbO + XS \rightarrow 2\,Pb + X + SO_2 \quad (12)$$

As a result, the residual As and Sb, part of Pb and the major part of Zn and Cd are scavenged into the air; Fe and Si are concentrated in Fe-rich slags that also incorporates sodium (Na), Mg and Al. The main purpose of this step is to pre-concentrate Ag in the form of Ag-rich Pb ore; the residual Ag is concentrated in Cu ore (Pernicka, 2014). Vaněk and Velebil (2007) distinguish two types of Cu ores: (i) Cu matte containing low amounts of Ag in the form of residual Ag_2S and Cu mostly as Cu_2S, and (ii) "black copper", a mixture of Ag, Cu, Pb and other metals. Last steps are cupellation (for the Ag-rich Pb) and liquation (Cu ore) which eliminate mainly the remainder of Sb, As, tin (Sn), Fe, Zn, and partly Cu and bismuth (Bi). These two proceeses are displayed in Figure 4.

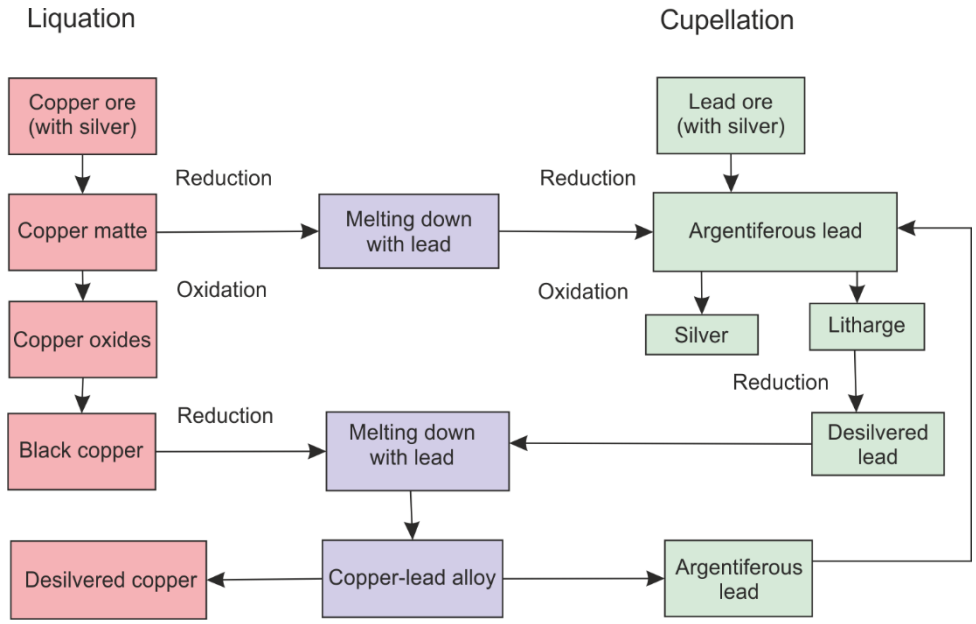

Figure 4. Processing of Ag-rich ores (according to Pernicka (2014)).

In summary, as a consequence of undergoing the smelting process, the major part of possible matrix elements is discarded either in the slag or into the air.

4.2 Separation methods

In general, the methods used for separating Ag from the matrix elements can be divided into two groups: (i) column chromatography methods, and (ii) precipitation methods.

The column chromatography methods are used for the vast majority of samples with the exception of silver coins. The used column chromatography methods (Kelly and Wasserburg, 1978; Kaiser and Wasserburg, 1983; Carlson and Hauri, 2001) inherit elution of Ag from exchange chromatography by 9 N HCl. However, if the residuum of HCl remains in the sample, it can lead to forming insoluble AgCl (Chapter 2.1) during the entire procedure. AgCl formed in such a way is insoluble in 15M HNO_3; consequently, it causes losses of Ag up to 25 %. Therefore, these previous methods were modified by Woodland et al. (2005), and a new elution strategy for Ag was introduced. The substantial difference in

the newly used method is in lowering amounts of HCl used during the procedure. In contrast to the previous methods, 0.5 mol/l HNO_3 was used for eluting Ag. This resulted in lower losses of Ag (Woodland et al., 2005).

Schönbächler et al. (2007) constituted three-stage ion-exchange chromatography to isolate Ag from terrestrial basalts and iron meteorite, which was adapted from Woodland et al. (2005). (Schönbächler et al., 2007) reported that the highest losses of Ag on first testing samples were 30 % due to the variations in the elution of Ag (consequences are stated in Chapter 4).

Precipitation of Ag with ascorbic acid is used for silver separation from silver coins (Stathis, 1948; Desaulty et al., 2011; Desaulty and Albarede, 2013; Albarède et al., 2016). The reaction scheme is stated below and is based on replacing Ag^+ in silver nitrate with H^+ resulting in the formation of Ag^0 and nitric acid (Equation 13).

$$2\,AgNO_3 + C_6H_8O_6 \rightarrow 2\,Ag + C_6H_8O_6 + 2\,HNO_3 \qquad (13)$$

The procedure of silver separation by the precipitation method differs in the literature. Stathis (1948) used between 11.2 mg and 137.6 of Ag and for precipitation he used 2 g of ascorbic acid per 100 ml of distilled water. Desaulty et al. (2011) used 200 mg of silver coin, precipitated by 0.15 N l-ascorbic acid which corresponds to 0.066 g per 100 ml; Desaulty and Albarede (2013) used the same procedure. Albarède et al. (2016) used ultrasonic leaching to obtain non-destructively Ag from coins, and the amounts thus gained Ag is not stated; for the precipitation is used 0.15 M ascorbic acid (2.64 g per 100 ml).

The further steps are similar for all three methods. They include drying and redisolving of the sample in distilled or deionised water to remove nitric acid. Moreover, except the method described by Desaulty et al. (2011), further heating of solution on either 90 to 100°C or on a hot plate set on 95°C for 20 minutes was done (Stathis, 1948; Albarède et al., 2016), respectively. The proportion of the added ascorbic acid into coin solutions was kept identical at 1:2 for all precipitation methods.

In the case of the first method (Stathis, 1948), after the addition of ascorbic acid, the solution was heated for 15 minutes, and further filtered, washed and ignited. In contrast, Desaulty et al. (2011) centrifuged the suspension and redissolved the precipitate in 5 ml of 15 M HNO_3, and no further heating was applied. The method developed by Albarède et al. (2016) included addition of ascorbic acid, followed by centrifugation, dissolution of the precipitate in 15 M HNO_3 and heated to dryness.

Brügmann et al. (2019) implemented column chromatography for archaeological samples containing low amounts of Ag, in particular gold nuggets.

An overview of the silver recovery rates from various previously used separation methods is given in Table 4.

Table 4. Selection of reported Ag recovery rates for published separation methods. They are listed according to a year of publication and type of the separation method.

Authors	Column separation	Precipitation
Kaiser and Wasserburg (1983)	lost for two samples, 70–100 %	
Carlson and Hauri (2001)	30 %, 41 %, 56 %, 75 % and 78 %*	
Woodland et al. (2005)	≥75 %	
Schönbächler et al. (2007, 2008)	~ 99 %	
Luo et al. (2010)	99.8 ± 2 % (2SD, n = 4)	
Junk et al. (2016)	80 ± 0.05 % (2SD)	
Guo et al. (2017)	96.47 ± 2.51 % (2SD, n ≥ 5)	
Argapadmi et al. (2018)	70 %, >90 % (majority of samples), and 85–100 % (Ag standards)	
Brügmann et al. (2019)	accepted yields ≥99 %	
Stathis (1948)		>99.9 %
Desaulty et al. (2011)		~ 99 %
Albarède et al. (2016)		>99.8 %

* recovery rates for single samples

4.3 Instrumentation and analytical techniques

Schönbächler et al. (2007) stated that the instrumental mass bias, compared with TIMS, is generally ten times higher for MC-ICP-MS. Nevertheless, corrections are capable to eliminate this mass bias effectively. Compared with TIMS, the use of the MC-ICP-MS due to different ionisation source enables to analyse elements with higher ionisation potential (Rehkämper et al., 2001).

Correction methods which are used for Ag isotopes are the standard–sample bracketing (SSB) and normalisation using Pd, due to similar masses with Ag. The most common isotopic pair used for corrections of instrumental fractionation is $^{108}Pd/^{105}Pd = 1.18899$ (Woodland et al., 2005; Schönbächler et al., 2007) but other ratios were also employed such as $^{110}Pd/^{104}Pd = 1.0604$ (Kelly and Wasserburg, 1978), and $^{108}Pd/^{106}Pd = 0.97238$ (Carlson and Hauri, 2001).

Schönbächler et al. (2007) mentioned that imprecision in measurement could also be induced by the presence of Cd which interferes with Pd masses 106, 108, and 110; in that case, correction by ^{111}Cd is required. However, Schönbächler et al. (2007) stated that correction by ^{111}Cd is unnecessary for Cd/Ag ratios up to 0.01.

Guo et al. (2017) focused on minimising the matrix effects caused by Zn, Pb, Cu and Fe by using specific Pd isotopic pair for normalisation; the one which does not form interferences with matrix elements. A series of experiments were performed which led to constraining the mass ratios of X/Ag, for which the selection of Pd isotopic pair would be sufficient to correct for matrix effects; Fe/Ag ≤ 600, Cu/Ag ≤

50, Pb/Ag ≤ 10, and Zn/Ag ≤ 1 were acquired as approximate threshold values. Compared to these approximated values for corrections by specific Pd isotopic pair, Schönbächler et al. (2007) stated that a ratio Zn/Ag = 0.1 does not require adjustments and corrections in measurement.

The terms external and internal normalisation are used differently through the literature. In one case the term internal normalization is perceived as normalization by isotope of the analysed element (e.g. Sr, Nd); and the external normalisation is perceived as normalization by element different from the one analysed but with similar characterisation to the one analysed (e.g. Pb/Tl) (Rehkämper et al., 2001; Woodland et al., 2005; Schönbächler et al., 2007). However, the term internal normalisation is also used in a broader sense. The term normalisation standard is used for an element used for mass bias corrections added into both, the sample and the isotopic reference material (Baxter et al., 2006; Luo et al., 2010). Brügmann et al. (2019) use the term Pd-doping and external bracketing to express addition of Pd into the reference solution used for bracketing. For purposes of this thesis, are used mass bias corrections by Pd or normalisation by Pd.

5 METHOD AND EXPERIMENTS

In this chapter sample preparation, silver separation, verification of the precipitation method, sample-standard bracketing and experiments with measurement of silver standard NIST SRM 978a are explored.

The instruments employed were the inductively coupled plasma optical emission spectroscopy (ICP-OES Agilent Technologies 5110), flame atomic absorption spectroscopy (FAAS VARIAN AA 280 FS), Neptune Plus high-resolution MC-ICP-MS (Thermo Fisher Scientific) and centrifuge (UNIVERSAL 320R, Hettich Zentrifugen).

5.1 Standard and Reference Materials

For isotopic measurements NIST SRM 978a was used, which was prepared from a high purity metal silver and nitric acid (Rasberry, 1984). The ratio is set to $^{107}Ag/^{109}Ag$ = 1.07638 (Rasberry, 1984; Rosman and Taylor, 1998). The NIST SRM 978a is the only certified isotopic standard of silver. To monitor the stability of the signal over time, NIST SRM 978a was measured repeatedly over an extended period: August 2018, January 2019, April 2019, May 2019, and July 2019 (Figure 18). Other silver-containing standards in which Ag isotopic compositions using MC-ICP-MC were determined were IAEA-S-1, IAEA-S-2, IAEA-S-3 (Chapter 2), JMC Spec pure Ag, and ASTASOL-Ag (ANALYTIKA Praha, CZ).

The reference materials used to establish the accuracy of the measurement with ICP-OES were SU-1b (CCRMP), ZW-C (CGS), and CCU-1e (CCRMP); the calibration reference material was ASTASOL-MIX (ANALYTIKA Praha, CZ). The reference material used for FAAS measurements was SU-1b. For mass bias corrections of Ag isotopic measurements on MC-ICP-MS Pd single stock solution ASTASOL Calibration Standard Solution (ANALYTIKA Praha, CZ) was used.

5.2 Samples

The method, as described by Desaulty et al. (2011), was performed on several archaeological samples. The highest obtained yields of 81 % showed that further tests are necessary. The specimens used for this purpose were sulphur standards IAEA-S1, IAEA-S2, and IAEA-S3, spectrographically standardised silver powder (Spec pure Ag by JMC, Limited England) and CZ 9001 (1N) (i.g. ASTASOL-Ag).

The real samples were Celtic coins from two oppida in Stradonice (central Bohemia) and Staré Hradisko (central Moravia) (Figure 5). The coin samples are dated back to 2nd to 1st century BC, more accurately 180–70 BC.

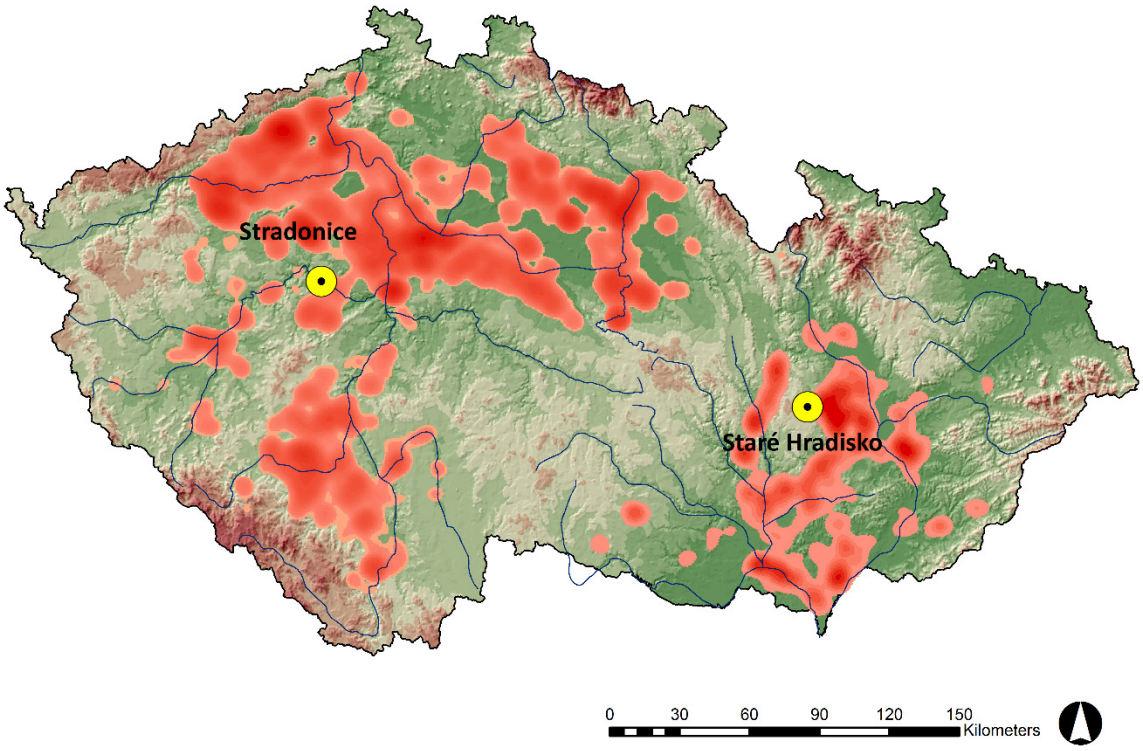

Figure 5. The density of the archaeological sites in the 2nd -1st century BC (red). The yellow dots represent the placers of Celtic coins. The map was built in ArcGIS and the density added by a Kernel density function (author: Mgr. Alžběta Danielisová, PhD.)

5.3 Reagents

The dissolution and sample separation were done in a class 10000 laminar flow-box (BLOCK DGP 1500). For sample preparation high-purity 2D nitric acid and de-ionised water (DIW) prepared by Academic Milli-Q Water Purification System (USA) purchased from Millipore Corporation with an electric resistance of 18.2 MΩ·cm and 25 °C were used. For precipitation of Ag ACS reagent L-ascorbic acid purchased from Sigma-Aldrich with the purity of ≥99 % and content of heavy metals ≤0.002 % established by ICP-OES was used.

5.4 Analytical procedure

The undermentioned method of silver separation for archaeological applications is based on the work of (Stathis, 1948; Desaulty et al., 2011; Albarède et al., 2016).

5.4.1 Dissolution

The specimens were precisely weighed on the Sartorius analytical scale by Sartalex. From the samples used for the tests of the method (Table 5) a stock solution that contained ~1 g of Ag on 100 ml of 2 % HNO_3 was created with the exception of the CZ 9001 (1N) that contained ~0.5 g of Ag per 100 ml of 2 % HNO_3. Twenty-five fragments of the Celtic coins were dissolved (Table 5), the weights of the coin samples were between 1.6 and 17.5 mg; with the average value of 6.3 mg and median 4.9 mg. From coin samples, a stock solution of 10 ml was prepared by the addition of 2 % HNO_3. For every set of samples, a blank sample was also prepared.

The Celtic coin samples were dissolved in Savilex beakers by addition of 5 ml of concentrated (15 N) HNO_3. The beakers were sealed and allowed to digest for 24–48 hours on a hotplate CERAN 500 set at 120-130 °C (Figure 6). The IAEA sulphur standards in the form of Ag_2S powder were dissolved in an equal manner as the coin samples; by 5 ml of concentrated HNO_3 and heated in closed Teflon beakers for 24–48 hours. The CZ 9001 (1N) in a liquid form was diluted to the required concentration. The JMC Spec pure Ag powder was dissolved with 15 M HNO_3 without heating; the observed reaction was exothermic, and the dissolution was accompanied by a change in colour. After this step, no visible residues were present, and the vial was further heated on a hot plate for 5 minutes on 125 °C.

Table 5. Summary of type and number of samples. Shown are also different concentrations of ascorbic acid.

Sample type	Compound	L-ascorbic acid (0.0037 M) [a]	L-ascorbic acid (0.028 M) [b]	L-ascorbic acid (0.15 M) [c]
IAEA-S1	Ag_2S (s)	3	3	3
IAEA-S2	Ag_2S (s)	3	3	3
IAEA-S3	Ag_2S (s)	3	3	3
JMC Spec pure Ag	Ag (s)	10	10	10
ASTASOL-Ag	Ag (l)	3	3	3
Celtic coins	Ag (s)	10		15

Note: [a] 0.066 g per 100 ml chosen according to (Desaulty et al., 2011); [b] 0.5 g per 100 ml lower medium value is chosen to observe the transition between low and high concentrations of the ascorbic acid, [c] 2.5 g per 100 ml chosen according to (Albarède et al., 2016).

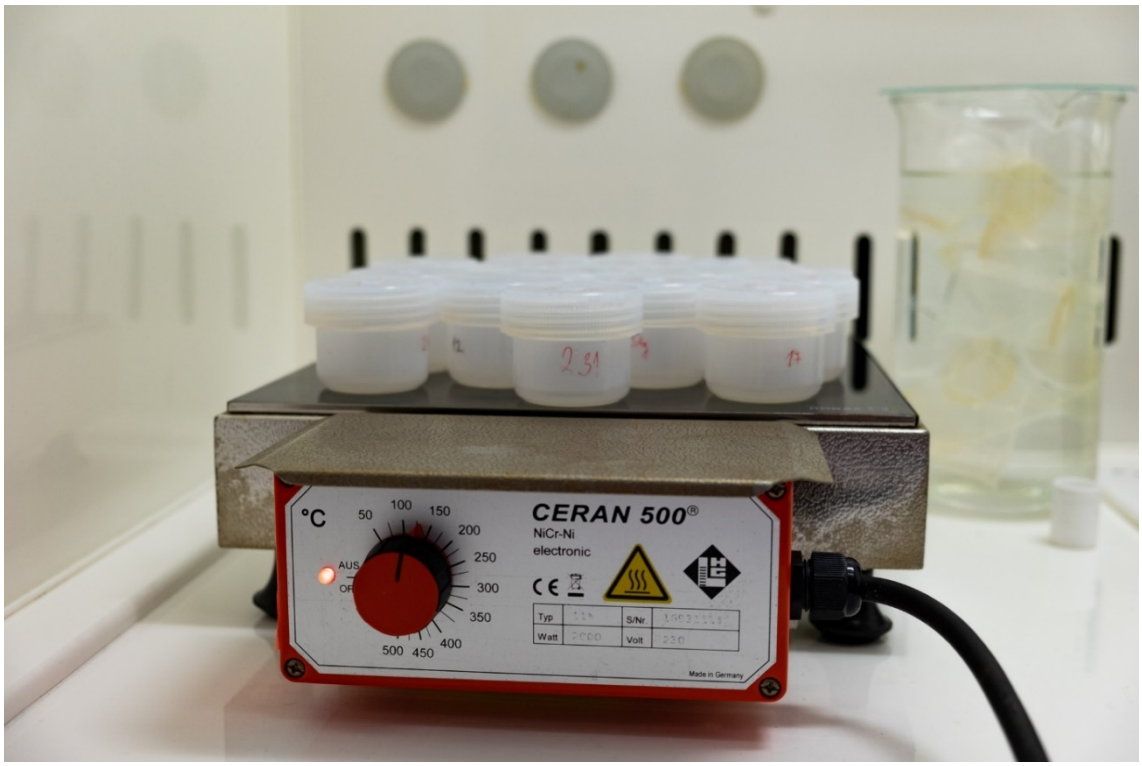

Figure 6. Samples dissolved on a hot plate in closed Savilex beakers at 120–130 °C for 24–48 hours.

5.4.2 Separation of silver – precipitation method

An aliquot of 5 ml from the stock solutions (Chapter 5.4.1) was kept on a hot plate set at 120 °C until the samples were completely dry (~3–6 hours). The dried samples were redissolved by addition of 15 ml DIW, and an aliquot of 100 µl was removed and filled up to 10 ml in a volumetric vial for measurements by ICP-OES.

The samples were heated on a hot plate for 20 minutes on 95 °C before the addition of 7 ml of freshly prepared L-ascorbic acid (further details are listed in next paragraphs), and again for 15 minutes after the precipitation of Ag by addition of L-ascorbic acid was proceeded. Thus created suspension with precipitated Ag was decanted into centrifugation vials (Figure 7) and centrifuged for 50 minutes at a rotation speed of 8500 rpm. The supernatant was decanted (pipetted in case of the coin samples precipitated by 0.0037 M L-ascorbic acid) and stored for further isotopic measurements, e.g. Cu, Pb. 5 ml of concentrated HNO_3 was added to the precipitated solid Ag in the centrifugation vial. This solution was returned to the original Savilex beaker from previous steps and reheated for 30 minutes on 120 °C.

To obtain Ag recovery rates of this method from the final solution, an aliquot of 100 µl for measurements on ICP-OES was removed. The final solution was stored in 20 ml glass vials in 2 % HNO_3.

In literature are used a significantly different concentration of ascorbic acid 2 g per 100 ml, 0.15 N which corresponds to 0.066 g per 100 ml, and 0.15 M which is 2.64 g per 100 ml (Stathis, 1948; Desaulty et

al., 2011; Albarède et al., 2016), respectively. Three different concentrations of L-ascorbic acid per 100 ml of DIW were tested: 0.066 g, 0.5 g and 2.5 g.

The final stage of precipitation displays Figure 7; the L-ascorbic acid is already added, and the samples are prepared for centrifugation.

Figure 7. The final stage of precipitation. The ascorbic acid is added, and the samples are prepared for centrifugation. The ascorbic acid powder prepared for dissolution in DIW and further used for precipitation of Ag is displayed in the upper right corner.

5.5 Instrumentation

5.5.1 ICP-OES and FAAS

All samples were measured by ICP-OES (operator: Ing. Věra Vonásková), and silver in some cases double-checked by FAAS (operator: Ing. Věra Vonásková). The analytical conditions of the measurements by ICP-OES are displayed in Table 6.

Table 6. Analytical conditions of the ICP-OES instrument.

Instrumental setting and analytical conditions	Values
Replicates	3
Pump speed	12 rpm
Uptake delay	15 s
Rinse time	20 s
Read time	10 s
RF power	1.20 kW
Stabilisation time	15 s
Viewing mode	radial and axial (dependent on the element)
Viewing height	8 mm
Nebulizer flow	0.70 L/min
Plasma flow	12.0 L/min
Aux flow	1.00 L/min

The elements were collected (Ag, Al, As, Bi, Ca, Cd, Co, Cr, Cu, Fe, Mn, Mo, Ni, Pb, Sb, Sn, Sr and Zn) in both radial and axial viewing mode and different wavelengths, the wavelength and viewing mode used for analysis differ for each element (Table 7).

Table 7. Detection limits and used wavelengths for the ICP-OES measurements.

Element	Viewing mode	Wavelength (nm)	Detection limits (mg/kg) *
Ag	Axial	328.068	5
Al	Radial	396.152	25
As	Axial	193.696	25
Bi	Axial	223.061	25
Ca	Radial	396.847	0.5
Cd	Axial	214.439	2
Co	Axial	230.786	5
Cr	Axial	267.716	5
Cu	Axial	327.395	5
Fe	Radial	238.204	2.5
Mn	Radial	257.610	0.5
Mo	Axial	202.032	5
Ni	Axial	216.555	5
Pb	Axial	220.353	15
Sb	Axial	206.834	15
Sn	Axial	189.925	1.5
Sr	Radial	407.771	1
Zn	Axial	206.200	1

Note: *DL calculated for 0.2 g per 100 ml, i.e. dilution factor of 500

The measurement conditions and instrumental setting of FAAS are noted in Table 8.

Table 8. Measurement conditions and instrumental setting of FAAS for measurements of Ag.

Instrumental setting and measurement conditions	Values
Instrument mode	Absorbance
Sampling Mode	Manual
Calibration Mode	Concentration
Wavelength	328.1 nm
Slit Width	0.5 nm
Gain	34 %
Lamp Current	6.0 mA
Lamp Position	2
Background Correction	On
Measurement Time	3.0 s
Pre-Read Delay	3 s
Flame Type	Air/Acetylene
Air Flow	13.50 L/min
Acetylene Flow	2.00 L/min
Burner Height	17.5 mm

Multielement calibration solution ASTASOL-MIX was used to construct a calibration curve with a correlation coefficient of 0.99999. The reference materials used for verification of measurement accuracy on ICP-OES were SU-1b, SY-4 and ZW-C (Table 10). The reference materials measured by FAAS were SU-1b and CCU-1e (Table 9).

Table 9. Values of Reference Materials measured by FAAS (values are listed in mg/kg).

		CCU-1e * Copper Concentrate	
Element	Measured Value (2SD, n = 2)	Status	Value
Ag	196.5 ± 10	Certified	205.2 ± 2

Note: * a concentrate of sulphide minerals

Table 10. List of used reference materials used for ICP-OES analysis (values are listed in mg/kg ± 2SD, n = 2).

	CCU-1e [b] Copper Concentrate			SU-1b Nickel-Copper-Cobalt Ore			ZW-C [a] Zinnwaldite	
Element	Measured Value	Status	Certified Value	Measured Value	Status	Certified Value	Measured Value	Working Value
Ag	201.8 ± 0.5	Certified	205.2 ± 2	5.5 ± 1.2	Certified	6.39 ± 0.12		–
Al	1652 ± 3	Certified	1385 ± 33	41475 ± 150	Certified	43000 ± 1000	94550 ± 1100	97600 ± 1400
As	998.8 ± 5.5	Certified	1010 ± 50	<25	Certified	2.49 ± 0.40	28.75 ± 0.50	31 ± 4
Bi				<25	Provisional	2.73 ± 0.70	<25	15 ± 2.8
Ca	1805 ± 3	Certified	1290 ± 50	18850 ± 120	Certified	22100 ± 600	2423 ± 76	2600 ± 100
Cd	76.5 ± 0.1	Certified	74.2 ± 2.6	6.75 ± 0.50	Inform.	3	<2	1.5 ± 1
Co	295.5 ± 0.1	Certified	301 ± 6	602.3 ±2.5	Certified	672 ± 13	<5	2 ± 0.5
Cr	6.25 ± 0.5	–	–	273.3 ± 0.5	Inform.	320	38 ± 15	56 ± 3.4
Cu	224900 ± 550	Certified	228800 ± 2400	10950 ± 100	Certified	11850 ± 140	43 ± 6	39 ± 2.8
Fe	310700 ± 650	Certified	307000 ± 5000	245700 ± 1050	Certified	255400 ± 2700	65580 ± 1850	66100 ± 700
Mn	92.75 ± 0.50	Certified	96 ± 7	670.8 ± 1.5	Certified	703 ± 19	6783 ± 316	7500 ± 160
Mo	13.75 ± 0.50	Provisional	16.1 ± 1.9	<5	Inform.	4	<5	4.3 ± 0.55
Ni	35.25 ± 10.50	Provisional	7.27 ± 0.64	19700 ± 100	Certified	19530 ± 170	15.25 ± 1.50	11 ± 4
Pb	6700 ± 1	Certified	7030 ± 120	53 ± 1	Certified	58 ± 5	50.25 ± 14.50	80 ± 5
Sb	80 ± 2	Certified	104 ± 7	<15	Inform.	0.2	<15	4.2 ± 0.9
Sn	<15	Indicative	15	–	–		– [c]	1300 ± 120
Sr	7.5 ± 0.1	Indicative	2	277.8 ± 1.5	Inform.	280	17.5 ± 1.0	17 ± 1.8
Zn	30250 ± 1	Certified	30200 ± 400	237.5 ± 23.5	Certified	235 ± 19	955.5 ± 76.0	1050 ± 40

Note: [a] Uncertified material, listed are solely working values; [b] a concentrate of sulphide minerals; [c] Sn does not qualitatively enter the solution.

5.5.2 MC-ICP-MS

The employed MC-ICP-MS (operators: RNDr. Jakub Trubač, PhD. and Petra Venhauerová) for isotopic measurements of Ag is Neptune Plus (Thermo Fisher Scientific, Bremen, Germany).

This high-resolution multicollector ICP-MS consists of three parts: the ICP module, the ESA module and the multicollector module (Figure 8). The ICP module is responsible for inlet and ionisation of the sample; it consists of an inlet system, plasma and ion generation devices. After the introduction of the sample in the nebuliser, an aerosol that contains a mixture of argon and sample is formed. In the spray chamber larger liquid particles are eliminated, and the subtilized aerosol is induced into the plasma torch where the sample is immediately ionised. The ESA (electrostatic analyser) module focuses and accelerates the beam through a system of lenses and slits. The multicollector module separates masses and detects ions; it consists of the magnet, the amplifier system, the optics, and the multicollector; for purposes of this measurements Faraday cups were employed.

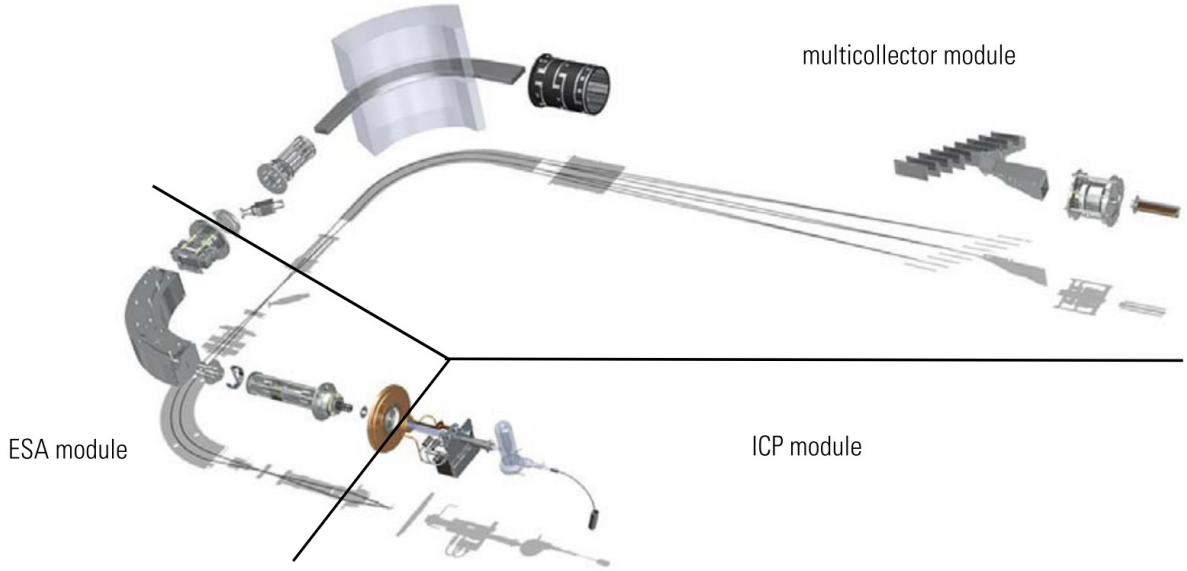

Figure 8. Segments of Neptune Plus MC-ICP-MS as specified in the Neptune Plus Hardware Manual (2009).

The standards and samples were introduced into the plasma by a PFA self-aspirating nebuliser with a nominal flow of 50 µl/min (Elemental Scientific, Omaha, NE, USA). The isotopes ^{105}Pd, ^{106}Pd, ^{107}Ag, ^{108}Pd and ^{109}Ag were collected on Faraday cups at L1, C, H1, H2 and H3 positions, respectively. The data acquisition parameters and operating conditions for Ag isotopic measurements are summarised in Table 11.

Wash time was adjusted manually for background intensities on cups of 0.0001 V.

Table 11. MC-ICP-MS operating conditions and data acquisition parameters.

Instrument setting and data acquisition parameters	Values
Rf Power	1200 W
Cool Gas	16.0 L/min
Auxiliary Gas	0.80 L/min
Sample Gas	1.067 L/min
X-Position	3.840 mm
Y-Position	3.060 mm
Z-Position	−4.750 mm
Peristaltic Pump	7.00 rpm
Sampler cone (nickel)	1.1 mm
Skimmer cone (nickel)	0.8 mm
Mass Scan Type	Continuous Mode
Intensity	~ 1.5V ^{107};^{109}Ag (100 ppb Ag)
Background (2 % (v/v) HNO_3	~ 0.04 mV for both ^{107}Ag and ^{109}Ag
Integration time	8.389 s
Idle time	3 s
Cycles/blocks	40/1

For the corrections of mass bias, the normalisation by Pd single stock solution, ASTASOL Calibration Standard Solution (ANALYTIKA Praha, CZ) was used. Even though different Ag/Pd ratios were tested (1:0, 1:1, 1:2, 1:8, and 1:20), the final ratio used was 1:1 (explained in Chapter 7.3). For corrections of the instrumental mass discrimination $^{108}Pd/^{105}Pd = 1.18899$ (Woodland et al., 2005; Schönbächler et al., 2007) was used, and $^{108}Pd/^{106}Pd = 0.97238$ (Carlson and Hauri, 2001) was also tested. Samples were measured in the sequence of NIST SRM 978a–Sample–NIST SRM 978a, both sample and bracketing standard contained 100 ppb of Ag and 100 ppb of Pd. The results are expressed in either $\varepsilon^{109}Ag$ or $\delta^{109}Ag$ (Equation 1 and 2, Chapter 2). For calculations of the ε and δ values, the average value of the bracketing standards is used.

The reference materials in which isotopic composition was measured were IAEA-S1, IAEA-S2, IAEA-S3, JMC Spec pure Ag, and ASTASOL-Ag. The reference materials prior to separation were measured in two repetitions, and the comparison to the published values is shown in Table 14. The Spec pure Ag and ASTASOL-Ag were also measured after the separation. Further, the isotopic composition of ASTASOL-Ag was measured in samples with various Ag yields to monitor possible fractionation during the separation process induced by incomplete recovery rates.

6 RESULTS

Measurements of silver isotopes come with several artefacts that need to be taken under consideration to ensure quality analysis and correct data outcome. Separation from matrix elements is required.

6.1 Characteristic of the samples and precipitation method

For silver isotopic measurements in archaeologic samples, fragments of coins found on the site were used or a small amount of sample from Celtic coins was removed. The removal was performed by chipping the edge of the coin to ensure that the historical value of coins would not be impaired. The weights of the Celtic coin samples obtained this way varied significantly and were between 1.6 and 17.8 mg (Figure 9). The mass of the majority of Celtic coin fragments was <5 mg (median 4.9 mg).

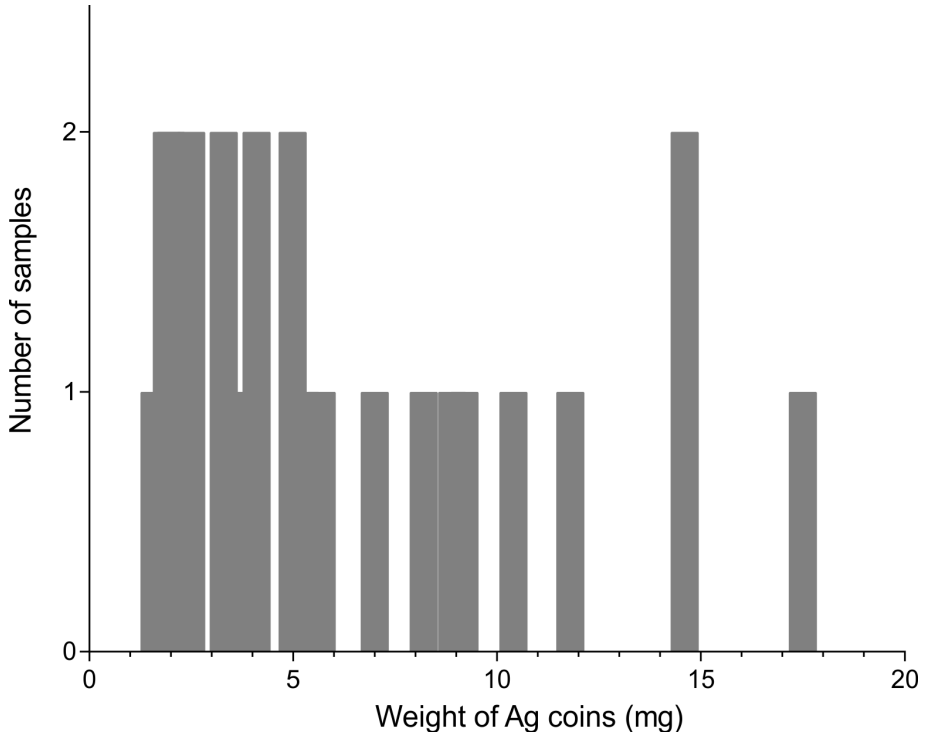

Figure 9. Distribution of the weights of Celtic coin samples.

The obtained samples were in the form of several small fragments per coin; the size of them was in the order of millimetres. An examination of the fragments under the Digital Microscope (Hirox RH-2000) was performed, and residual particles of mineral grains were observed together with the samples of coins (Figure 10).

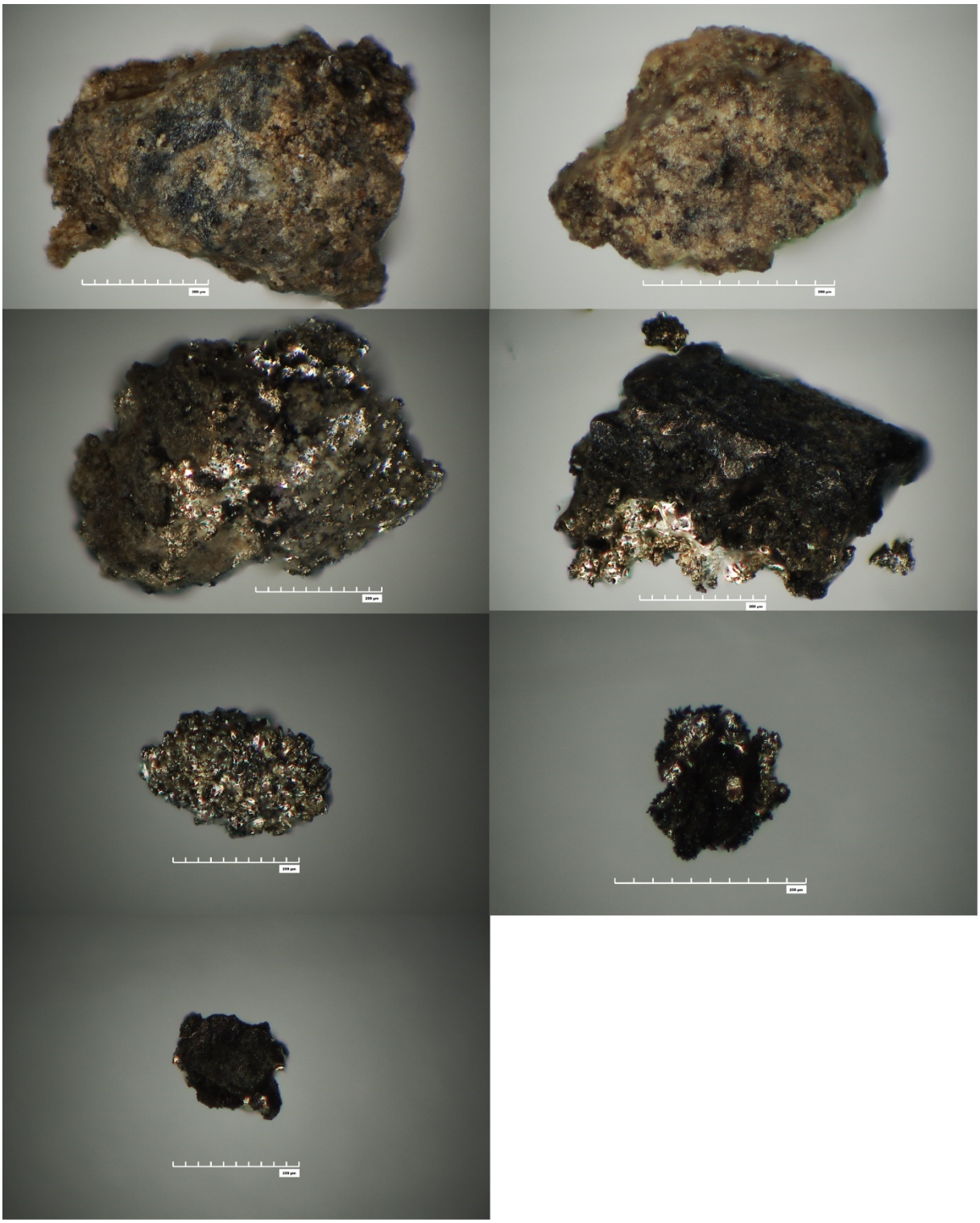

Figure 10. Photos of fragments before dissolution in concentrated nitric acid made by Digital Microscope Hirox RH-2000 at the Institute of Criminalistics, Police of the Czech Republic. The scale is set on 200 µm and the stepping motor on scanning with step 3 µm/pulse. On the top row are photos of mineral grains presented among sample fragments.

All fragments were dissolved and measured using ICP-OES. The elements measured by the ICP-OES (Ag, Al, As, Bi, Ca, Cd, Co, Cr, Cu, Fe, Mn, Mo, Ni, Pb, Sb, Sn, Sr, and Zn) were chosen to determine the presence and concentration of matrix elements that could cause analytical artefacts during measurements on the MC-ICP-MS. The Celtic coin samples were largely made of Ag (median 98 %), with subordinate amounts of Cu with median value of 2 %, followed by Pb which was detected in 10 coins out of 25 with a median value of 0.2 % (Figure 11) (Note: ICP-OES detection limit for Pb is <15 mg/kg).

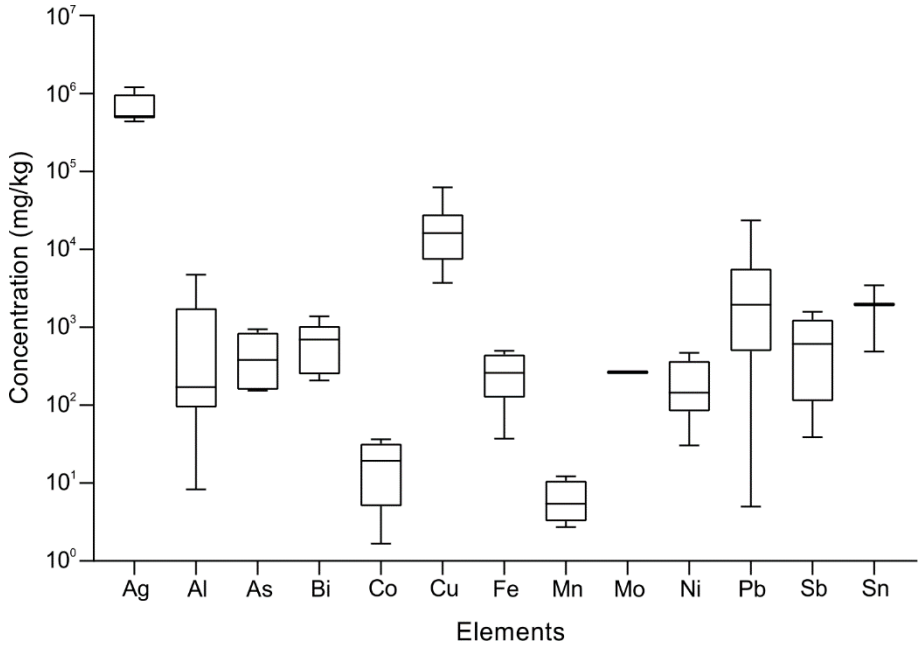

Figure 11. Box plot of selected elements in the Celtic coins after their dissolution in concentrated HNO_3. The concentration values for Al, Co, and Pb in one measurement were below the detection limit of the ICP-OES. Therefore, these three values were estimated as one-third of the elements` detection limit: 8.34 mg/kg, 1.67 mg/kg, and 5 mg/kg for Al, Co, and Pb, respectively. Each box represents the lower and upper quartile, and the line inside the box median (the middle quartile); whiskers represent the minimum and maximum concentration values.

6.2 Separation method

In order to ensure accurate and precise measurements by the MC-ICP-MS, the silver present in Celtic coins needed to be separated from other matrix elements. For this purpose the precipitation method applied for separation of Ag from archaeological samples was used.

6.2.1 Testing samples

Series of experiments on the reference materials was performed. The employed standards were IAEA-S1, IAEA-S2, IAEA-S3, JMC Spec pure Ag (Limited England) and ASTASOL-Ag (ANALYTIKA Praha, CZ). The tests of the effectiveness were performed with three different concentrations of the L-ascorbic acid: 0.15 M, 0.028 M, and 0.0037 M; and on three different original

masses of Ag: 5 mg, 2.5 mg, and 0.45 mg. The Ag precipitation reaction is expressed by Equation 13 (Chapter 4.2).

Several obstacles appeared during the procedure. After addition of the L-ascorbic acid into the diluted samples, colour change appeared almost immediately with positive correlation towards amounts of Ag and the strength of the acid. However, the colour change of the samples precipitated by equal molarity acid, containing identical amounts of silver, was immense (Figure 13). In samples that contained 0.45 mg of Ag, subtle colour change appeared only for samples precipitated by highly concentrated acid whereas at lower molarities, the colour change was basically invisible. With decreased amounts of Ag present, it became more difficult to decant the supernatant. The precipitate after centrifugation was in the form of floating fine particles or fragmental "pellets" inside the supernatant or floating on the surface.

The highest yields of 97 ± 3 % were obtained for 5 mg of silver precipitated by the 0.15 M L-ascorbic acid. The second was 5 mg precipitated by the 0.0037 M L-ascorbic acid (94 ± 3 %) and the 2.5 mg precipitated by the 0.028 M L-ascorbic acid (94 ± 1 %) (Figure 12).

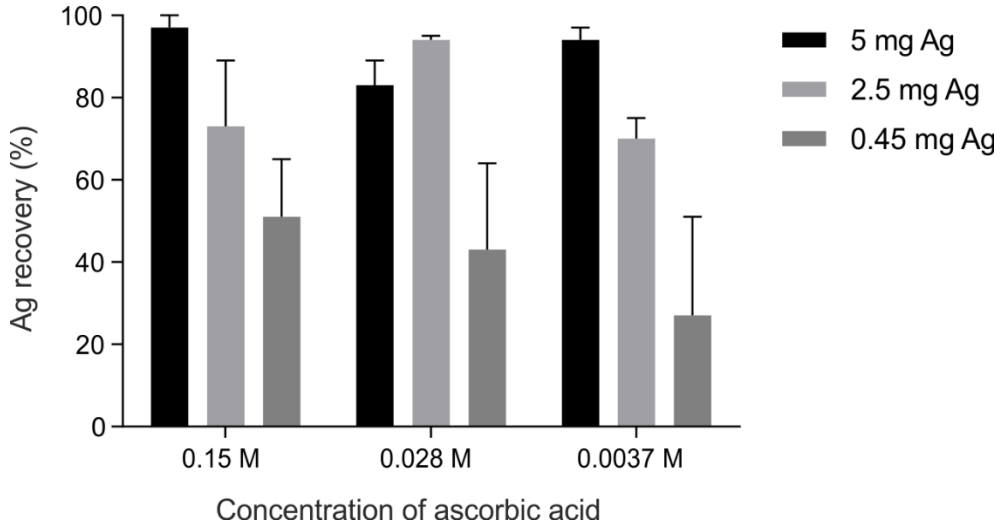

Figure 12. Performed tests of the precipitation method, the dependence of Ag recovery rates and amounts of silver prior to precipitation. The tests differ in amounts of precipitated Ag and the concentration of the used ascorbic acid. The amounts of the precipitated Ag were 5 mg, 2.5 mg, and 0.45 mg for the Spec pure Ag, ASTASOL-Ag, and IAEA-S1, IAEA-S2 and IAEA-S3, respectively.

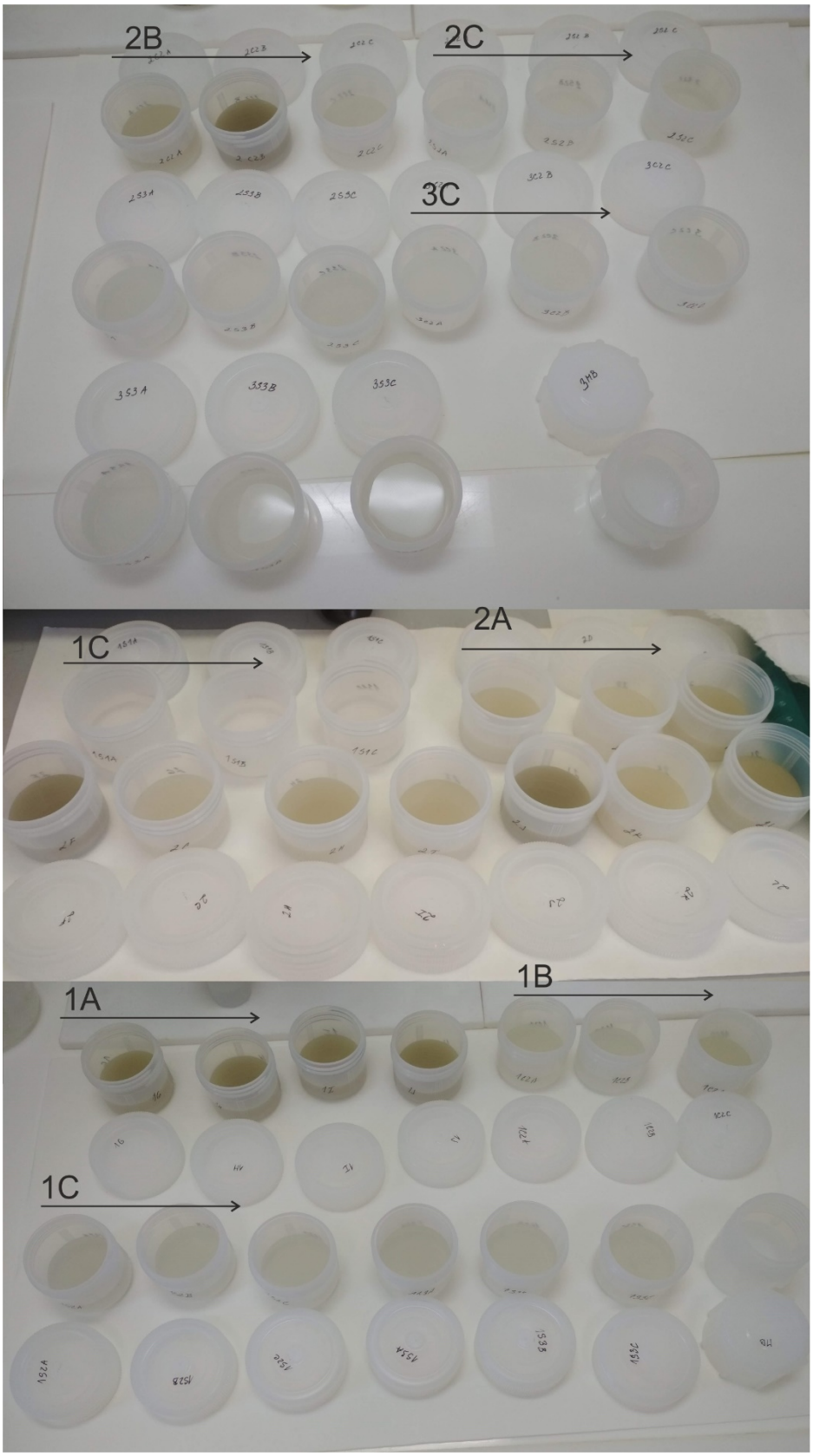

Figure 13. Colour changes in some of the samples after the addition of the ascorbic acid. The number signalises the acid concentration (1 – 0.15 M, 2 – 0.028 M, and 3 – 0.0037 M) and letters the amount of Ag in the solution (A – 5 mg, B – 2.5 mg, and C – 0.45 mg).

6.2.2 The Celtic coin samples

The fragments of Celtic coins were precipitated with 0.0037 M (ten samples, first set) and 0.15 M (fifteen samples) L-ascorbic acid. The colour change after the addition of the 0.15 M ascorbic acid differs significantly in its intensity and rapidity (Figure 14). The amounts of Ag present in each sample differed, and concentrations measured by ICP-OES before and after the separation process are stated in Table 13.

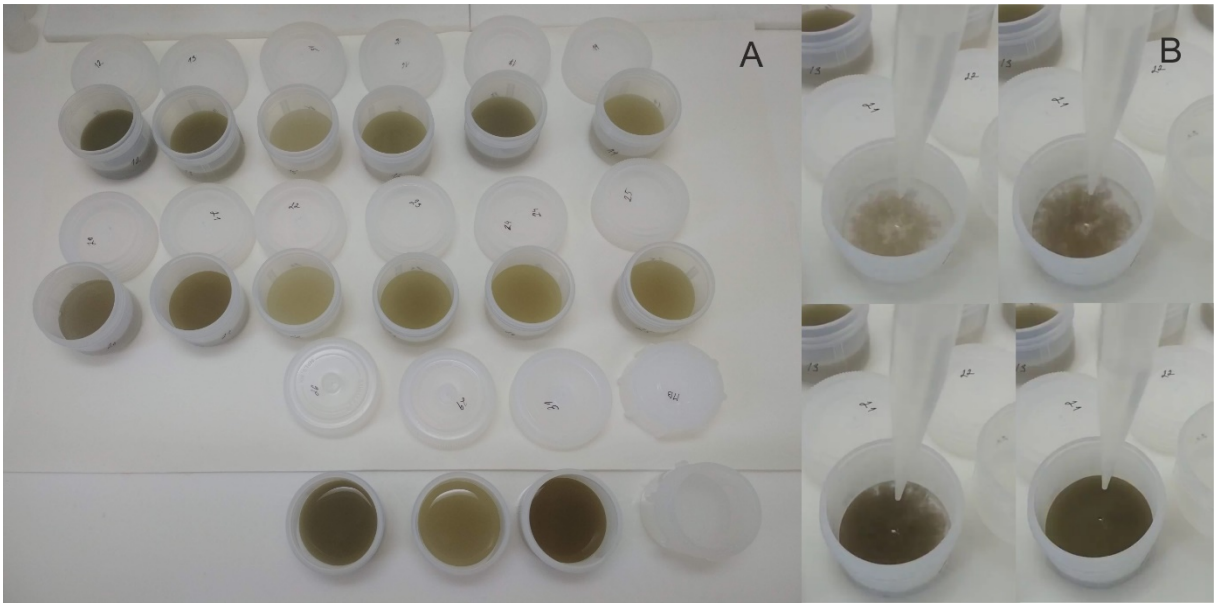

Figure 14. [A] final colour of Celtic coin fragments after addition of ascorbic acid; [B] the colour change in a sample containing 4.6 mg of Ag during 2 seconds while adding 0.15 M ascorbic acid. The amounts of Ag present in each sample are stated in Table 13; the number on the Savilex beaker corresponds with the Working Sample ID in the first column (mince_x). The samples on the [A] picture are arranged in the ascending order starting by 12 and ending by 31; the last beaker is a blank sample.

In the separated Celtic coin samples, after precipitation of Ag, the majority of the concentrations of matrix elements remained in the supernatant. In the precipitate, a residual amount of Bi, Cu and Fe and in one sample Ni remains together with Ag (Figure 15).

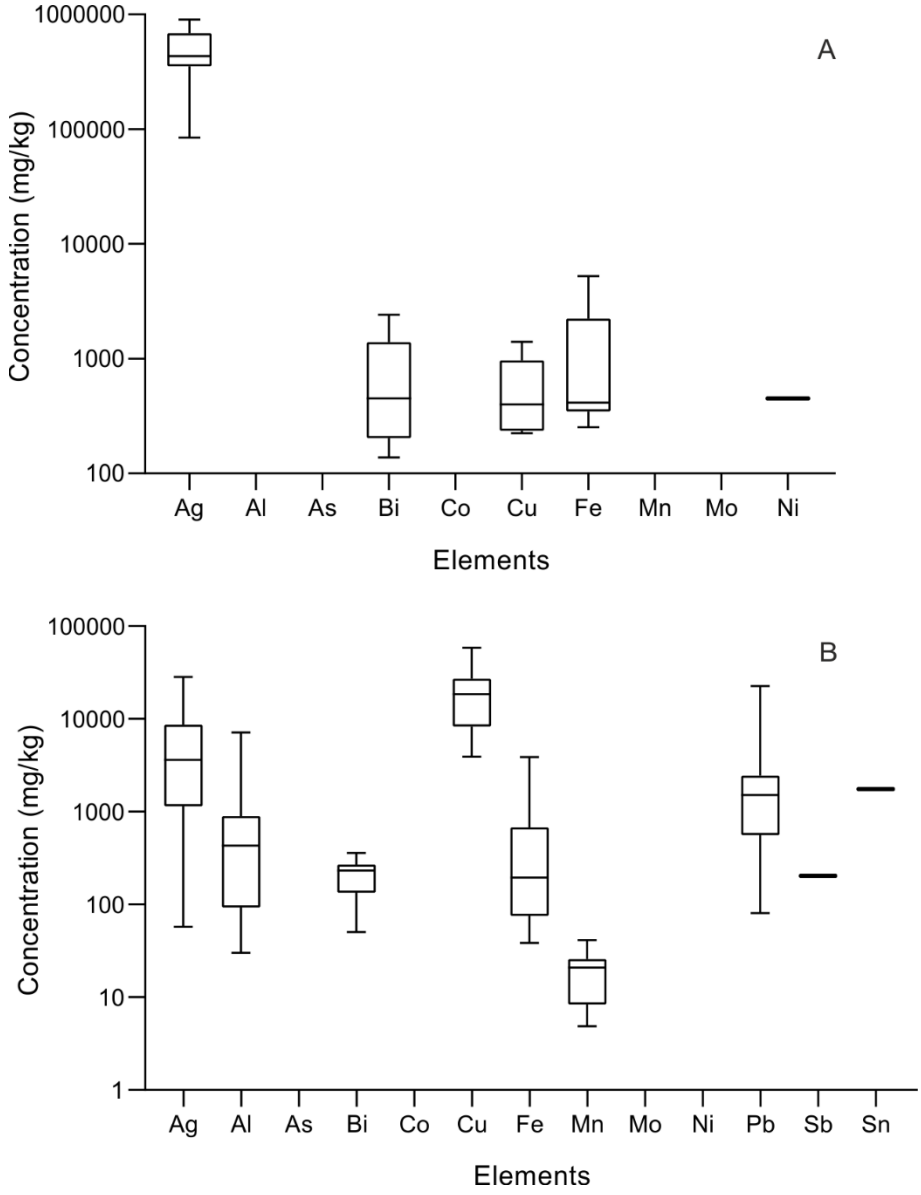

Figure 15. Effectiveness of separation Ag from other elements; [A] concentrations of elements present in the precipitate, [B] concentrations of elements in the supernatant after precipitation of Ag. Each box represents the lower and upper quartile. The line inside the box represents the median concentration value. Whiskers represent the minimum and maximum concentration values. Included are data from all 25 coins samples regardless of the concentration of the ascorbic acid used for precipitation.

The correlation between Ag recovery rates and the original weights of Celtic coin samples and the amounts of Ag after precipitation was expressed (Figure 16).

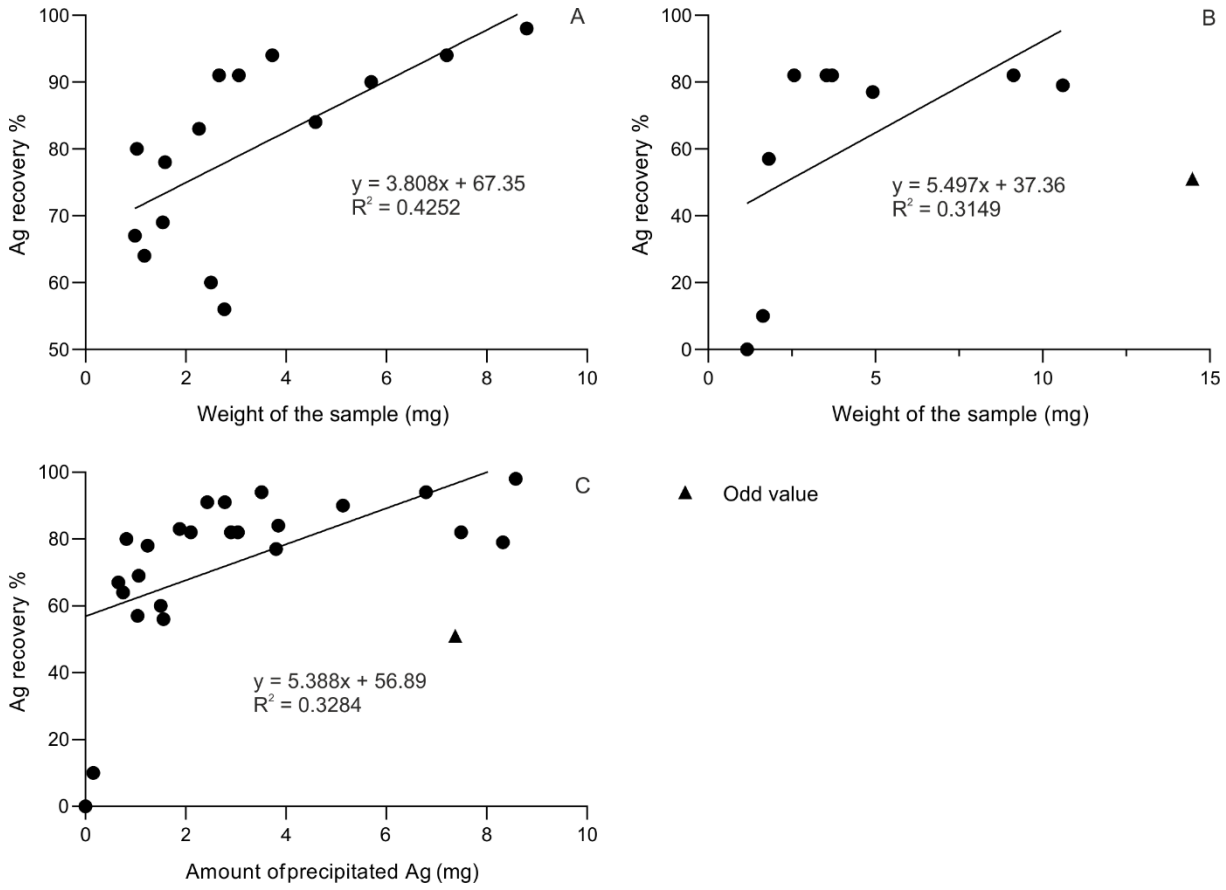

Figure 16. [A, B] Correlation between the weight of the sample and Ag recovery; [A] samples precipitated by 0.15 M ascorbic acid, [B] samples precipitated by 0.0037 M ascorbic acid. [C] Correlation between amounts of precipitated Ag and percentage Ag recovery. Included are values both from precipitation by 0.15 M and 0.0037 M ascorbic acid. Triangle symbol represents one distinct value excluded from the calculations of R^2 and equation.

6.3 Measurements of the isotopic composition of silver

Prior to the determination of the isotopic composition of coins, the testing of suitable instrumental setting was required. The NIST SRM 978a was measured with variable ratios of Ag/Pd: from pure Ag through Ag/Pd = 1:1; 1:1.5; 1:2; 1:8 to 1:20 (Figure 17). The pure uncorrected Ag (100:0 ppb) shows distinct values of $^{107}Ag/^{109}Ag$ = 1.04148 and lower XX. Usage of mass bias correction factor for $^{108}Pd/^{106}Pd$ yields systematically lower ratios of $^{107}Ag/^{109}Ag$ compared to those calculated using $^{108}Pd/^{105}Pd$. The ratios of $^{107}Ag/^{109}Ag$ for different ratios of Ag/Pd are in agreement; however, the Ag/Pd = 1:8 yields slightly lower values and the highest standard deviation.

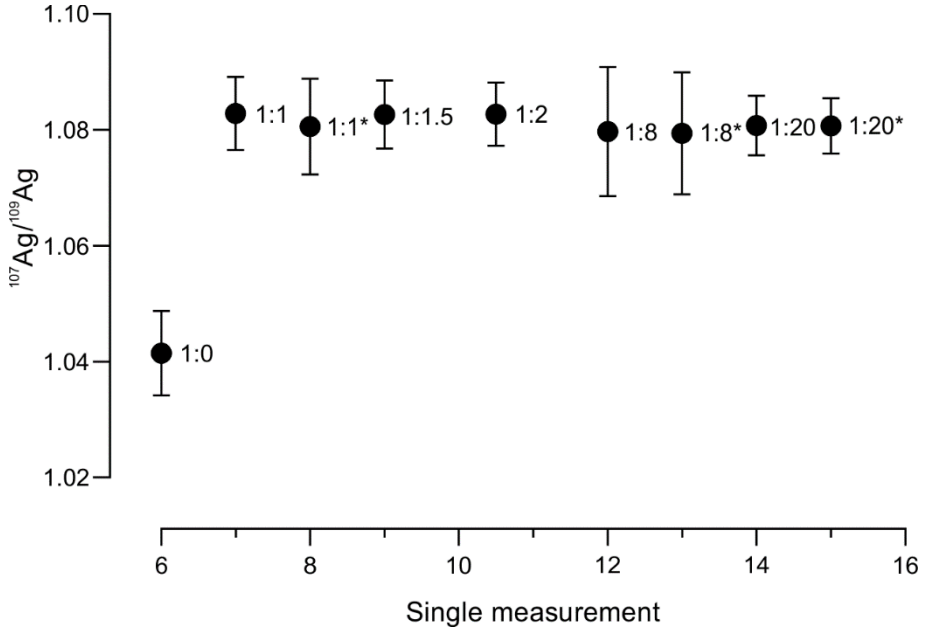

Figure 17. Variations caused by different ratios of Ag/Pd (the amount of NIST SRM 978a is constantly 100 ppb, and variations are in amounts of added Pd). The marked values (*) are corrected with the mass bias correction factor for $^{108}Pd/^{106}Pd = 0.97238$ (Carlson and Hauri, 2001). The other data points are corrected by the mass bias correction factor for $^{108}Pd/^{105}Pd = 1.18899$ (Woodland et al., 2005; Schönbächler et al., 2007).

The ratio of $^{107}Ag/^{109}Ag$ for the NIST SRM 978a remained stable over an extended period of time (Figure 18). The values oscillated between 1.08105 ± 0.00378 and 1.08088 ± 0.00719 over seven months.

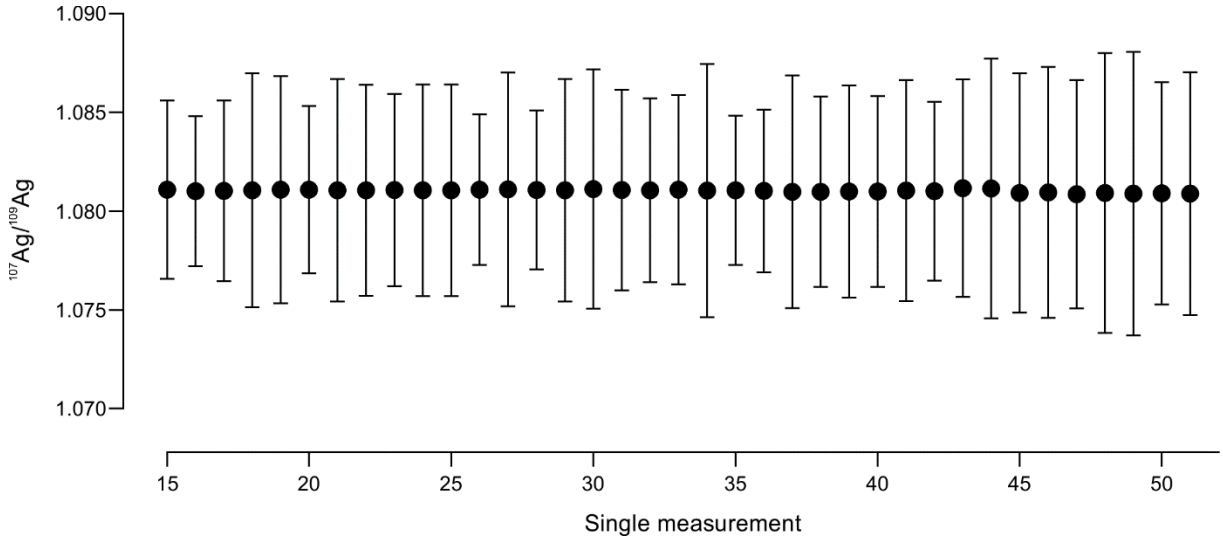

Figure 18. Isotopic measurements of the NIST 987a used for bracketing. The long-term reproducibility of the $^{107}Ag/^{109}Ag$ ratios obtained by MC-ICP- MS. Included are values measured over the period of seventh months, specifically January 2019, April 2019, May 2019, and July 2019.

6.3.1 Reference materials

The measured δ^{109}Ag value of NIST 987a is −0.003 ± 0.018, calculated was out of the values used for bracketing.

The Ag isotopic composition of reference materials for sulphur (IAEA-S1, IAEA-S2, and IAEA-S3) was measured in unseparated samples. The δ values of silver reference materials: ASTASOL-Ag (CZ 9001) and JMC Spec pure Ag were measured in samples prior to and after separation in samples with Ag recovery rates of 95 % and 98 %, respectively (Table 12).

Table 12. Measured isotopic composition of reference materials.

Reference Material	Description	ε^{109}Ag (2SD)
JMC Spec pure Ag	Spectrographically Standardised Silver Powder	1.03 ± 0.39 [a] 0.49 ± 0.22 [b]
ASTASOL-Ag (CZ 9001)	Calibration Standard Solution	0.87 ± 0.09 [a] 0.21 ± 1.49 [b]
IAEA-S1	Silver Sulphide	0.56 ± 0.01 [a]
IAEA-S2	Silver Sulphide	2.28 ± 0.08 [a]
IAEA-S3	Silver Sulphide	2.25 ± 1.25 [a]

Note: [a] isotopic composition measured in unseparated samples (n = 2), [b] isotopic composition measured in samples after separation (n = 1)

For verification of fractionation during the separation process, were used testing samples of single stock solution ASTASOL-Ag that contained 2.5 mg of Ag precipitated by all tree tested concentrations of ascorbic acid. The recovery rates of Ag were among 50 and 95 %. The ε values ranged between 0.207 ± 0.075 and 0.817 ± 0.011 (Figure 19).

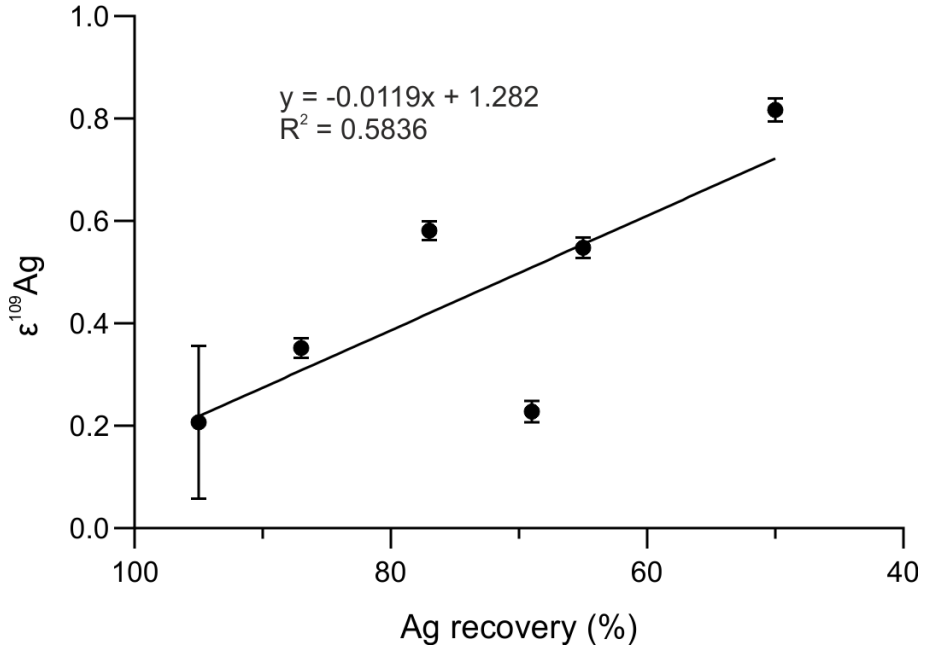

Figure 19. Correlation between the isotopic composition of ASTASOL-Ag and recovery rates of Ag.

6.3.2 Isotopic composition of coins

The presence of elements that could cause possible matrix and spectral interferences during isotopic measurement was tested by ICP-OES; Zr and Pd further by ICP-MS (operator: Doc., RNDr. Ladislav Strnad, PhD.), due to low detection limits and lower measurement sensitivity of ICP-OES. The concentration of Pd and Zr measured in samples diluted to contain 100 ppb of Ag were <0.02 ppb and <0.05 ppb, respectively.

Due to the absence of Cd in the samples, correction of mass bias by ^{111}Cd was not required. The mass bias correction factor of $^{108}Pd/^{105}Pd = 1.18899$ was used to correct samples and standard $^{107}Ag/^{109}Ag$ ratios, applied was an exponential correction law. The samples were measured in a sequence of NIST SRM 978a-sample-NIST SRM 978a and for calculations of the ε was used the average of these ambient NIST SRM 978a values.

The final $\varepsilon^{109}Ag$ values for Celtic coins ranged between -1.589 ± 0.012 and 0.746 ± 0.011 (Table 13).

Table 13. Summary of the measured values for the Celtic coins.

Working ID	Sample ID	ε^{109}Ag		2SD	Type (period)	Ag recovery (%)	Original Ag (mg)	Precipitated Ag (mg)
mince_1	H5-257 7 [a]	–1.497	±	0.013	- (LT D1)	9	1.635	0.160
mince_2	H5-257 716 [a]	–1.589	±	0.012	Stradonice (LT D1)	50	14.482	7.375
mince_4	H5-257 720 [a]	0.052	±	0.012	Stradonice (LT D1)	81	9.127	7.490
mince_5	H5-257 722 [a]	0.171	±	0.008	Stradonice (LT D1)	77	10.605	8.325
mince_6	H5-257 725 [a]	–1.311	±	0.014	Stradonice (LT D1)	55	1.815	1.040
mince_7	H5-257 726 [a]	0.334	±	0.007	Stradonice (LT D1)	80	3.535	2.900
mince_8	H5-257 727 [a]	–0.241	±	0.010	Stradonice (LT D1)	79	2.574	2.100
mince_9	H5-257 728 [a]	–0.509	±	0.008	Stradonice (LT D1)	80	3.707	3.040
mince_10	H5-257 733 [a]	0.339	±	0.009	Stradonice (LT D1)	76	4.918	3.805
mince_12	H5-257 736 [b]	0.341	±	0.007	Stradonice (LT D1)	98	8.799	8.580
mince_13	H5-257 740 [b]	0.405	±	0.011	Stradonice (LT D1)	94	3.728	3.516
mince_15	H5-257 743 [b]	0.335	±	0.009	Staré Hradisko (LT D1)	56	2.771	1.560
mince_16	H5-257 745 [b]	0.108	±	0.010	Staré Hradisko (LT D1)	90	5.697	5.136
mince_17	H5-257 746 [b]	0.427	±	0.014	Staré Hradisko (LT D1)	91	3.060	2.780
mince_19	H5-257 753 [b]	0.746	±	0.011	Staré Hradisko (LT D1)	60	2.504	1.502
mince_20	H5-257 754 [b]	–0.216	±	0.012	Staré Hradisko (LT D1)	67	0.989	0.660
mince_21	H5-257 755 [b]	0.433	±	0.009	Staré Hradisko (LT D1)	84	4.584	3.848
mince_22	H5-257 760 [b]	0.689	±	0.009	Stradonice/Karlstein (LT D1)	64	1.178	0.750
mince_23	H5-257 761 [b]	0.139	±	0.011	Stradonice/Karlstein (LT D1)	78	1.587	1.244
mince_24	H5-257 762 [b]	0.076	±	0.008	Stradonice/Karlstein (LT D1)	91	2.666	2.428
mince_25	H5-257 763 [b]	–0.132	±	0.010	Stradonice/Karlstein (LT D1)	80	1.026	0.818
mince_26	H5-257 765 [b]	0.326	±	0.009	Stradonice/Karlstein (LT D1)	94	7.200	6.790
mince_29	H5-257 771 [b]	0.267	±	0.009	Stradonice/Karlstein (LT D1)	69	1.544	1.064
mince_31	H5-257 773 [b]	0.368	±	0.011	Stradonice/Karlstein (LT D1)	83	2.262	1.878

Note: [a] Ag separated by low concentrated ascorbic acid (0.0037 M); [b] Ag separated by high concentrated ascorbic acid (0.15 M); LT D1 ~180–70 BC

7 DISCUSSION

7.1 Evaluation of the precipitation method

The separation of silver by precipitation method is consistently applied for silver coin samples. Further, the reaction of silver nitrate with ascorbic acid is used as staining reaction for determination of the presence of ascorbic acid in animal organs (Gough and Zilva, 1933) and preparation of ultrafine silver particles or AgNPs (Wu and Meng, 2005; Rashid et al., 2013).

Previous studies applied this method for samples that contained between 11.2 and 137.6 mg (with a median value of 72.5 mg) (Stathis, 1948), or 200 mg of silver (Desaulty et al., 2011). Albarède et al. (2016) introduced leaching of the coins instead of their dissolution, in order to not damage the historical value of the coin, and do not state the amounts of silver thus obtained.

The original weight of Celtic coin samples ranged between 1.6 and 17.8 mg (median 4.9 mg) (Figure 9). However, these values are influenced by the presence of mineral grains among the fragments of silver coins (Figure 10). Therefore, the more critical information is given by the amount of Ag in the solution prior to precipitation. These values in the Celtic coin samples were between 0.99 mg and 14.48 mg with a median value of 2.8 mg. The comparison of median values for amounts of Ag used by Stathis (1948) and Desaulty et al. (2011) with the median concentration of silver in Celtic coin samples gives 26 and 71 times lower weights, respectively. Owing to that evaluation of suitability of this method for such low amounts was necessary.

The precipitation reaction, expressed by Equation 13, is based on the reaction of L-ascorbic acid with silver nitrate in a solution. After addition of the L-ascorbic acids a greyish precipitate forms and remains in the suspension. A further step is centrifugation of the suspension in order to sediment the precipitated Ag. Even though the centrifugation time was 50 minutes and the rotation speed 8500 rpm, the precipitated Ag did not sediment entirely. The fine precipitated particles of Ag remained segregated in the suspension even after this step and either formed the goldish colour of the suspension or “coat” on the surface layer of the supernatant.

In some cases, the centrifugation led to the formation of aggregates of the precipitate “pellets” that floated in the solution but too fine-grained to be able to sediment. Overall, the variable proportion of the particles generated by the precipitation was low in size and unable to sediment with gravitation force. This step is most likely the main cause that leads to the majority of the Ag loss. Wu and Meng (2005) described the characteristics of the precipitation products (metallic Ag) based on the conditions during precipitation. They aimed to produce ultrafine Ag powder and observed dependence of precipitated size particles on the pH and temperature. The larger particle sizes were observed during typical room temperatures (23°C) and at lower pH (around 2). Further, Wu and Meng (2005) postulated that the speed

of the reaction rate influenced the final particle sizes, the slower the reaction, the higher the coalesce intensity. This could explain the obtained results for the performed test and Celtic coin samples.

One of the possible solutions how to improve the yields can be to include filtration of the suspension through fine filters, from which the Ag would be removed by HNO_3 or ignited as used by Stathis (1948) for separation of Ag from Ag–Cu alloys. However, it is important to note that this can introduce contamination by other elements which may result in matrix effect or build spectral interferences for isotopic measurements. Another and perhaps more suitable adjustment would be to implement findings by Wu and Meng (2005): (i) to eliminate heating prior to addition of L-ascorbic acid, (ii) add the acid at rather slowly rate, (iii) do not reheat the solution and (iv) leave it intact for at least half an hour prior to centrifugation.

The results do not suggest a significant correlation between the content of silver and the strength of the ascorbic acid used for precipitation (Figure 12); slightly correlates higher effectiveness of precipitation with higher concentrated L-ascorbic acid for 0.45 mg of Ag. However, the error bars are significant, and the variation in the Ag recovery rates can be influenced by the size of particles formed by precipitation.

The overall visible trend for Ag recovery is dependence on the amount of precipitated silver (Figure 16). The dependence among Ag recovery of Celtic coin samples and the amount of silver present prior to precipitation gives slopes of 3.808 and 5.497 with $R^2 = 0.4252$ and $R^2 = 0.3149$, for 0.15 M and 0.0037 M ascorbic acid, graph A and B, respectively. Moreover, the overall trend that combines Ag recovery and amount of precipitated Ag for both concentrations of the acid results in a slope of 5.388 ($R^2 = 0.3284$). The higher amount of scattered points for the precipitation by 0.0037 M in graph B can be explained by loss of silver after centrifugation, induced by pipetting these ten samples. The fine floating particles that were not able to sediment and stayed in the suspension adhesively stuck to the surface of the tip. Therefore, further samples were decanted.

The silver coins are produced from native silver or minerals that contain silver which undergo smelting process. Elements constituting primary minerals with Ag are predominantly Pb, S, As, and Sb (summarised by Fujii and Albarede, 2018). The historical smelting process is summarised in Chapter 4.1.2, and during this process, significant amounts of matrix elements considerably decrease their concentrations. The percentage of silver in each coin compared with other present elements is 98 % (median value). The other elements measured by ICP-OES (Al, As, Bi, Ca, Cd, Co, Cr, Cu, Fe, Mn, Mo, Ni, Pb, Sb, Sn, Sr, and Zn) were present in subordinate concentrations; the second most frequent element was Cu (median 2 %). Stathis (1948) described that the presence of Pb, Cu, Bi, Cd, Ni, and Zn in the solution does not result in problems with precipitation of Ag.

In the precipitate residual amount of Bi, Co and Fe and in one sample Ni remained together with Ag. No observable dependence between Ag recovery rates of Celtic coin samples and the presence of other

elements occurred. The elements unsuitable for analysis by ICP-OES, due to low detection limits and lower measurement sensitivity of ICP-OES, which could cause possible spectral interferences with masses of Ag or Pd during the isotopic measurements on the Neptune Plus MC-ICP-MS were Zr and Pd. Therefore, the ICP-MS was used to obtain concentrations of these elements in the Celtic coin samples diluted to the Ag concentration of 100 ppb, which was used for Ag isotope determinations. The concentration in such diluted samples was below 0.02 ppb and 0.05 ppb for Pd and Zr, respectively. These concentrations do not influence the accuracy and precision of the MC-ICP-MS measurement (Schönbächler et al., 2007).

To conclude, the precipitation method showed to be an effective way of separation of silver from other matrix elements. The amounts of possible matrix elements in the final solutions were low, and their average concentration values compared with the ones of silver were lower by more than three orders of magnitude (Figure 15). The obtained results for the tests and Celtic coin samples showed an effective separation of Ag in higher concentrated samples. Subsequently, the yields can be improved by adjusting the method according to the findings of Wu and Meng (2005).

7.2 Isotopic composition of reference materials

The δ^{109}Ag value for NIST SRM 987a calculated from the measured ratios of ^{107}Ag/^{109}Ag used for bracketing coin samples is –0.003 ± 0.018 that corresponds with the value mentioned by Brügmann et al. (2019) at –0.004 ± 0.007 for NIST SRM 978a measured as an unknown sample and δ^{109}Ag = 0.005 ± 0.033 for NIST SRM 978a after ion exchange procedure (Argapadmi et al., 2018).

The Ag isotopic composition of isotopic standards for sulphur (IAEA-S1, IAEA-S2, and IAEA-S3) was measured in unseparated samples (Table 14). The δ^{109}Ag values for IAEA-S1 correspond with published value by Guo et al. (2017). However, the δ^{109}Ag values for IAEA-S2 and IAEA-S3 differ by one order of magnitude. These distinct values can be explained by the incomplete dissolution of these two reference materials (Ag_2S powder) in HNO_3. While the IAEA-S1 dissolved entirely within 24 hours, in the IAEA-S2 and IAEA-S3 solution few microscopic particles even after heating in Teflon beaker for over four days were visible. The matrix elements detected in this isotopic standard by ICP-OES were by four orders of magnitude lower compared with silver, which should not strongly influence the final δ^{109}Ag values (Schönbächler et al., 2007).

The δ values of ASTASOL-Ag (CZ 9001) and JMC Spec pure Ag were measured in samples prior and after separation, the Ag recovery rates of separated samples were 95 % and 98 %, respectively. The discrepancy among the Ag isotope compositions in separated and unseparated samples of JMC Spec pure Ag and ASTASOL-Ag can be caused by the presence of matrix elements that could influence the precision and accuracy of the measurement. Nevertheless, the content of present elements in this reference materials was not measured. Considering the measured isotopic composition of

ASTASOL-Ag, samples with lower recovery rates (87 %, 77 %, 69 %, 65 %, and 50 %) do not suggest such extensive fractionation (Figure 19).

Furthermore, the measurement error for the IAEA-S3 is substantial and overall can be said that the measurement section of these reference materials (Table 14, excluding the IAEA-S1 measured in the previous section) was accompanied by observable instability in the signal.

Table 14. Comparison of measured and publishes δ^{109}Ag values (by Guo et al. (2017)) of the reference materials.

Reference Material	Description	Prague δ^{109}Ag (2SD)	Published data δ^{109}Ag (2SD, n ≥ 4)
JMC Spec pure Ag	Spectrographically Standardised Silver Powder	0.103 ±0.039 [a] 0.049 ± 0.022 [b]	No published data
ASTASOL-Ag (CZ 9001)	Calibration Standard Solution	0.087 ± 0.009 [a] 0.021 ± 0.149 [b]	No published data
IAEA-S1	Silver Sulphide	0.056 ± 0.001 [a]	0.020 ± 0.011 [a]
IAEA-S2	Silver Sulphide	0.228 ± 0.008 [a]	–0.029 ± 0.005 [a]
IAEA-S3	Silver Sulphide	0.225 ± 0.125 [a]	–0.027 ± 0.006 [a]

Note: [a] isotopic composition measured in unseparated samples (n = 2), [b] isotopic composition measured in samples after separation (n = 1)

7.3 MC-ICP-MS instrumental and analytical evaluation

The mass bias correction factor for ^{108}Pd/^{106}Pd = 0.97238 yielded systematically lower ratios of ^{107}Ag/^{109}Ag (Figure 17), and the corrected ratios of ^{107}Ag/^{109}Ag were highly scattered in comparison with the ratios corrected by isotopic pair ^{108}Pd/^{105}Pd = 1.18899. Further, the correction factor using ^{108}Pd/^{106}Pd showed a higher instability of the signal (Figure 20). Therefore, for calculations of final δ^{109}Ag and ε^{109}Ag values the correction factor using ^{108}Pd/^{105}Pd ratio systematically used in more recent studies was used.

Different Ag/Pd ratios were tested (Figure 21). Guo et al. (2017) compared different ratios and stated that the best linear relation between the natural logarithm of ^{109}Ag/^{107}Ag and ^{105}Pd/^{104}Pd gives a ratio of Ag/Pd = 1:20. However, while testing different ratios, the 1:8 resulted in higher measurement error and systematically lower final values of ^{107}Ag/^{109}Ag, and the 1:20 proved to cause unnecessarily high intensities of signal and extensive washing times. The ratios of Ag/Pd: 1:1, 1:1.5, and 1:2; resulted in a similar measurement error and the precision of ^{107}Ag/^{109}Ag values. Therefore, the samples were diluted on Ag/Pd ratios of approximately 1:1 or slightly higher prior to measurement by MC-ICP-MS.

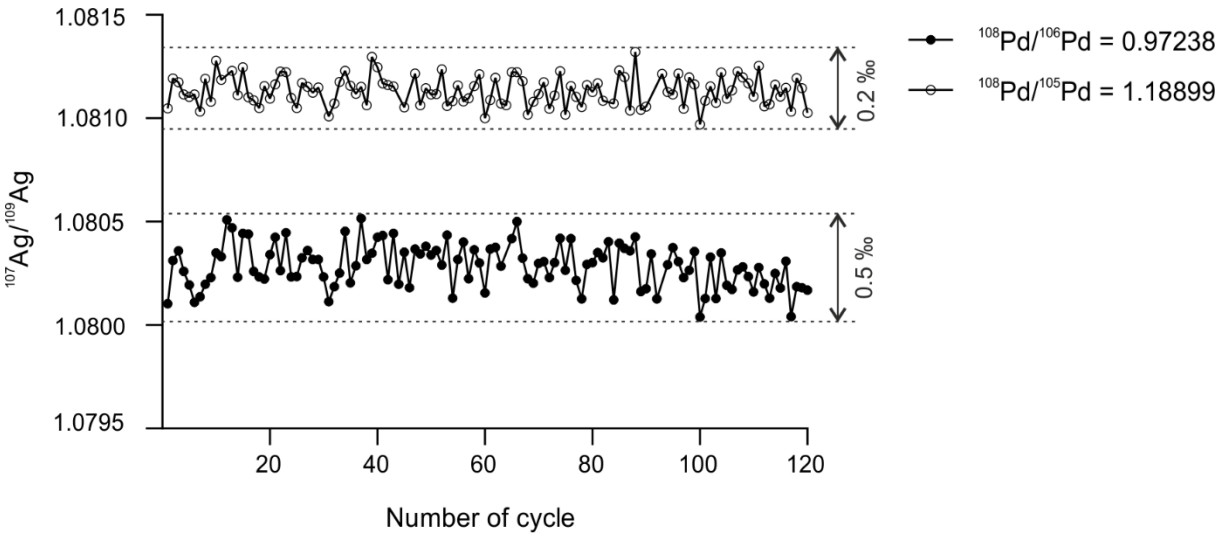

Figure 20. Comparison of different mass bias correction factors. The values were measured for NIST SRM 978a over three acquisition blocks. The mass bias correction factor for $^{108}Pd/^{106}Pd = 0.97238$ used by Carlson and Hauri (2001) and $^{108}Pd/^{105}Pd = 1.18899$ is used in later studies (Woodland et al., 2005; Schönbächler et al., 2007).

The measured ratio for the NIST SRM 978a clustered around $^{107}Ag/^{109}Ag = 1.08105 \pm 0.00007$. The certified value of this isotopic standard is 1.07638 ± 0.00022 (Powell et al., 1981) and further measured ratios for this isotopic standard are: 1.07916 ± 0.00052 measured by Plasma-54 MC-ICP-MS (Carlson and Hauri, 2001), 1.08048 ± 0.00042 measured by Nu Plasma MC-ICP-MS (Woodland et al., 2005), 1.07911 ± 0.00027 (Schönbächler et al., 2007)and 1.07976 (Schönbächler et al., 2008) measured by Axiom MC-ICP-MS, and 1.07959 ± 0.00018 measured by Neptune (Chugaev and Chernyshev, 2012) (Figure 21).

The long-term stability of the isotopic ratio for NIST SRM 978a is significant (Figure 18), and the bracketing procedure is sufficient to yield accurate and precise data.

The precision obtained for a single measurement section is ± 0.04 ‰ (2SD) which is in agreement with previously stated precisions for Ag isotopic measurements: ± 0.13 ‰ (Carlson and Hauri, 2001), ± 0.2 ‰ (Woodland et al., 2005), ± 0.05 ‰ (Schönbächler et al., 2007), ± 0.05 ‰ (Yang et al., 2009), and ± 0.015 ‰ (Luo et al., 2010).

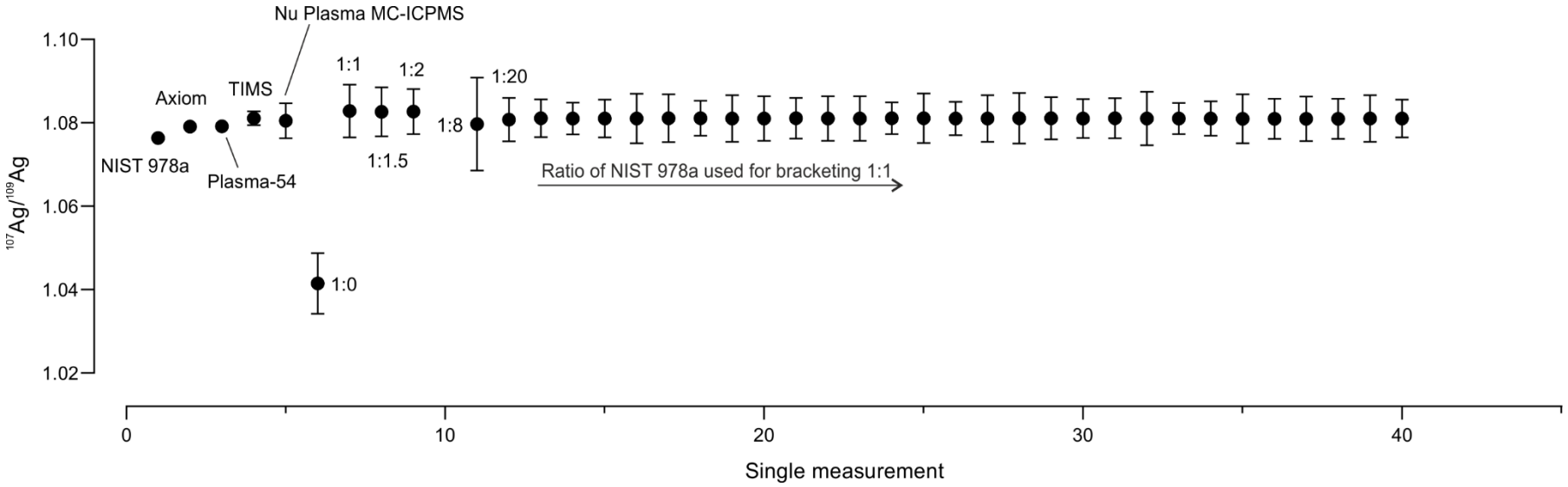

Figure 21. Published and measured data for the NIST SRM 978a, included tests with the Ag/Pd ratios (the amount of Ag was always 100 ppb, and the amounts of Pd was variable) and long-term reproducibility of the bracketing standard measurements (included values from January 2019, April 2019 and May 2019).

7.4 Fractionation due to separation

The results obtained for the isotopic composition of samples with yields of 95 %, 87 %, 77 %, 69 %, 65 %, and 50 % suggest possible fractionation during the separation process resulting in a shift of 0.1 ε units per 10 % decreased recovery. Compared to the fractionation observed by Schönbächler et al. (2007) during column chromatography, where the difference among first eluted 70 % and residual 30 % amounted to 5 ε units values, the one observed by precipitation method is rather minor. Fujii and Albarede (2018) argued the validity of the final values measured for samples after column chromatography separation with yields below 100 % due to extensive fractionation (~2.85 ‰) between Ag^+ and $AgCl^0$.

When calculating fractionation rates for both methods, the precipitation method leads to a shift of 0.1 ε units per 10 % decreased recovery (slope of –0.0119), and the one calculated from the shift in the isotopic composition caused by incomplete yield during column chromatography observed by Schönbächler et al. (2007) results in a shift of 1.7 ε units per 10 % decreased recovery. Considering that a substantial part of the ε^{109}Ag values of silver coins fluctuates around 0 and most of the values falls into ± 1 ε (Fujii and Albarede, 2018), the shift in ε values of 0.17 per 1 % induced by column chromatography is significant. However, the measured ε values for the variable Ag recovery rates in this study are highly scattered ($R^2 = 0.584$), and furthermore, the measurements were performed without replications. Therefore, for accurate conclusions and estimation of exact fractionation rate induced by uncomplete yields during precipitation of silver by L-ascorbic acid is required further and substantial research. The research would require measurement of a higher density of recovery rates and a statistically significant amount of repetitions for each sample.

Although the results imply modes Ag isotope fractionation during precipitation, this separation method compared to the column chromatography has proven to be suitable for archaeological samples that contain sufficient amounts of silver.

7.5 Isotopic composition of Celtic coin samples

The placer of measured Celtic coins is Bohemia or Moravia, and they come from Celtic tribes, specifically Boii (Gallic tribe). The Celtic coin samples are dated back to 180–70 BC. The obtained ε^{109}Ag values correspond with the published data (Figure 22); the distinct values around - 1.5 were measured for yields ≤55 % and are thus incorrect and misleading.

The obtained isotopic ratios were employed to perform two statistical tests introduced for the isotopic composition of historical silver coins by Fujii and Albarede (2018). The statistical tests were performed on a data set from which samples with Ag yields below 64 % were removed. The removed ε^{109}Ag values for yields below 56 % showed distinctive values: –1.497 ± 0.013, –1.589 ± 0.012, and –1.311 ± 0.014,

compared with so far published values of ε^{109}Ag for historical coin samples (Desaulty et al., 2011; Desaulty and Albarede, 2013; Albarède et al., 2016) (Figure 22). In contrast, the measured ε^{109}Ag values of Celtic coins for yields of 60 % and 56 % show no immediately apparent disparity in the ε^{109}Ag values, 0.746 ± 0.011 and 0.335 ± 0.009, respectively.

On the remaining data set the non-parametric Mann-Whitney U-test (compared are values of two unpaired groups) and paired parametric t-test (Table 15), with significance level $\alpha = 0.05$, were performed. The published data (Desaulty et al., 2011; Desaulty and Albarede, 2013; Albarède et al., 2016) were separated into time- and area-dependent groups: Antic West and East Mediterranean, Post-Columbian Spain, Medieval and Post-Medieval Europe; in total was compared published values. Due to the age and placement of Celtic coin samples, the measured ε^{109}Ag values for coins originating from America and Post-Columbian Spain were not included in the statistical tests.

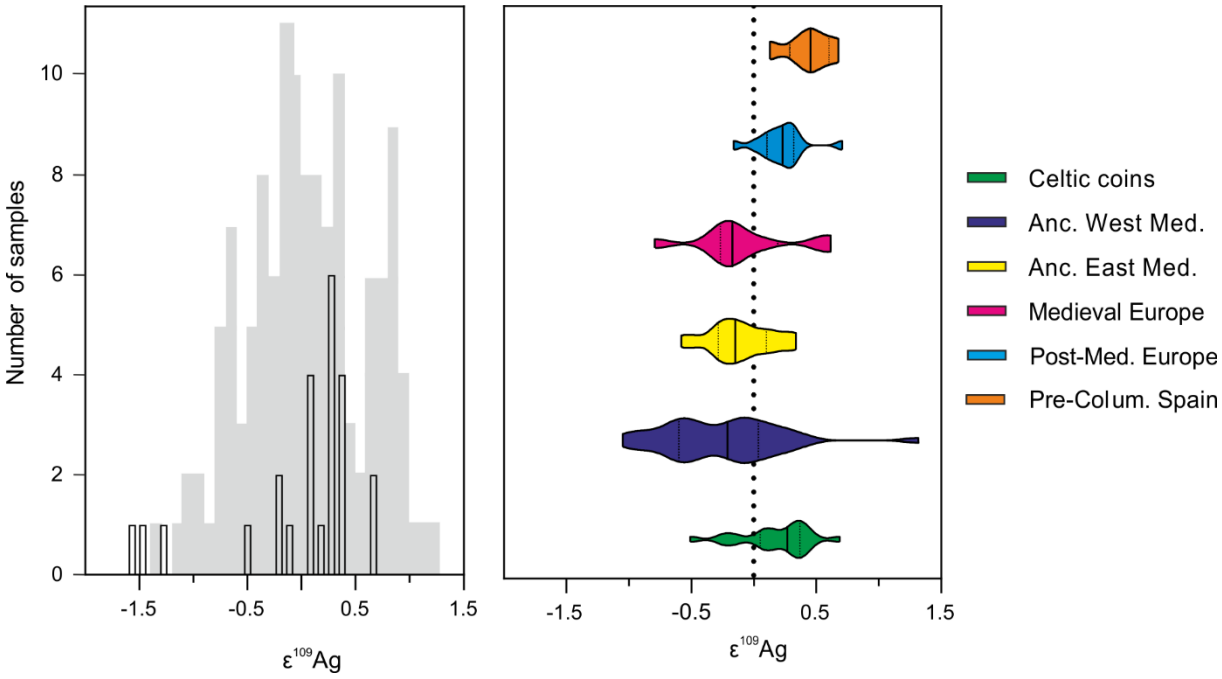

Figure 22. Isotopic composition of measured Celtic coin samples compared with published data (Desaulty et al., 2011; Desaulty and Albarede, 2013; Albarède et al., 2016). The grey area on the histogram symbolises distribution and density of published ε values (Fujii and Albarede, 2018) and the black bins across are measured ε values for Celtic coin samples. The intervals used for Celtic coin samples were chosen to correspond with the published data. The violin plot on the right shows the distribution of the data separated into time- and area-dependent groups; these groups were employed in the performed statistical tests (Table 15). The filled line inside the box represents the median value, and the dotted lines represent lower and upper quartiles. The ends of the violin plot represent minimal and maximal ε values. The smoothing of the violin plot is set on medium.

The group of Central Europe Celtic coins includes measured ε^{109}Ag in this study; the values range between –0.509 ± 0.008 and 0.689 ± 0.009. The correlations are expressed by the p-values; the values close to zero signify no correlation among the two evaluated areas and with larger values, the probability of correlation increases. The only more significant correlation of 0.86 for U-test and 0.63 for t-test, respectively, show the Celtic coins with the isotopic composition of coins from Post-Medieval Europe

(second half of 16th and 17th century). The comparison with the other three groups indicates uncommon origin.

There are several hypotheses about the origin of silver used for the coinage of Celtic coins from this era (based on Waldhauser (2003), Militký and Karwowski (2013), Murillo-Barroso et al. (2016), Wood et al. (2019) and consultation with A. Danielisová): 1. remelted Antic coins from the Mediterranean area, specifically former Carthaginian mines in Spain, 2. Germany, remelted coins or artefacts from Bavaria (specifically the late Iron Age sites like the oppidum of Manching) 3. exploitation of local deposits – Příbram, Kutná Hora (so far no evidence), and 4. Slovakian Ore Mountains. The performed statistic tests question the first hypothesis and do not imply any dependence among the source areas of Mediterranean and Celtic silver, i.e. exploitation of the same deposit type.

Nevertheless, for better understating and interpretation of the Celtic coins` isotopic composition comparison with a larger dataset would be required.

Table 15. Performed statistic tests on the isotopic composition of coins. The Celtic coins are measured samples in this thesis from which are excluded ε values of samples with Ag recovery <64 %. Other isotopic data are published data (Desaulty et al., 2011; Desaulty and Albarede, 2013; Albarède et al., 2016) sorted according to the area and timing. Listed values are p-values from two statistical tests: paired parametric t-test and non-parametric Mann-Whitney U-test. The larger p-values imply similar source area.

t-test	Aver		Std	CE Celtic coins	Anc. West Mediterr.	Anc. East Mediterr.	Medieval Europe	Post-Medieval Europe	Pre-Columbian Spain
Cent. E. Celtic coins	0.21	±	0.30	1	0.00	0.00	0.06	0.63	0.05
Anc. West Mediterranean	–0.25	±	0.47	0.00	1	0.23	0.30	0.00	0.00
Anc. East Mediterranean	–0.10	±	0.25	0.00	0.23	1	0.84	0.00	0.00
Medieval Europe	–0.08	±	0.39	0.04	0.30	0.84	1	0.03	0.01
Post-Medieval Europe [a]	0.22	±	0.19	0.63	0.00	0.00	0.03	1	0.04
Pre-Columbian Spain	0.44	±	0.17	0.05	0.00	0.00	0.01	0.04	1

Mann-Whitney U- test	CE Celtic coins	Anc. West Mediterr.	Anc. East Mediterr.	Medieval Europe	Post-Medieval Europe	Pre-Columbian Spain
Cent. E. Celtic coins	1	0.00	0.00	0.07	0.86	0.03
Anc. West Mediterranean	0.00	1	0.17	0.36	0.00	0.00
Anc. East Mediterranean	0.00	0.17	1	0.98	0.00	0.00
Medieval Europe	0.07	0.36	0.98	1	0.02	0.02
Post-Medieval Europe [a]	0.86	0.00	0.00	0.02	1	0.03
Pre-Columbian Spain	0.03	0.00	0.00	0.02	0.03	1

Note: [a] later half of the 16th century and 17th century

8 CONCLUSIONS

The precipitation method consistently applied for separation of silver in coin samples proved to be an effective way to disjoin silver from other matrix elements. In a minimal portion of the solutions stayed residual amounts of Cu, Bi, Fe, and in one sample Ni; however, these amounts are low compared to the content of silver and therefore do not influence the precision of isotopic measurement.

The ε^{109}Ag values obtained for Celtic coins are in agreement with the so far published ε^{109}Ag values for historical coins. Two statistical tests (t- and U-test) comparing ε^{109}Ag values measured for Celtic coin samples and published data sorted according to time- and area dependent groups were performed. One of the hypotheses about the origin of Celtic silver is that the metal came from the Mediterranean area. However, the p-values obtained from the performed statistical tests do not suggest a common metal source of Celtic and Mediterranean coins.

The Ag recovery rates were sufficient, and do not suggest significant dependence among the concentration of the used ascorbic acid and the amounts of silver precipitated. The overall visible trend that the Ag recovery rates seem to depend on is the amount of silver prior to precipitation. The step that may lead to lower recovery rates is the separation of the precipitate from the supernatant. The silver, due to low particle sizes created by precipitation, stayed in suspension and did not agglomerate even after intensive centrifugation. The sizes of silver particles formed by precipitation might be enlarged by adjustments in the method used (e.g. temperature, pH, the speed of ascorbic acid addition). However, these adjustments may not successfully secure a higher recovery for deficient amounts of silver prior to precipitation, and column chromatography may have to be applied.

The adjusted setting for measurements of silver isotopes using Neptune Plus MC-ICP-MS proved long-term stability of the obtained ^{107}Ag/^{109}Ag ratios for the NIST SRM 978a. The compared mass discrimination correction factors for different Pd isotopic pairs showed a slight difference in the corrected ^{107}Ag/^{109}Ag ratios. The ^{108}Pd/^{106}Pd correction pair yielded systematically lower ratios compared the ^{108}Pd/^{105}Pd and further resulted in lower stability of the signal leading to an oscillation of the corrected ^{107}Ag/^{109}Ag ratio by 0.5 ‰.

Examination of possible fractionation due to incomplete silver recovery rates during separation by precipitation method implies that the fractionation rate is modest (~0.1 ε units per 10 % decreased recovery) compared to the one induced by column chromatography (~1.7 ε units per 10 % decreased recovery). However, further research is needed to understand better and precisely estimate fractionation among different separation methods.

To conclude, although the tested method comes with certain restrictions; it is an effective way of separating Ag in order to ensure accurate and precise isotopic data for archaeological samples.

REFERENCES

Albarède F., Blichert-Toft J., Rivoal M. and Telouk P. (2016) A glimpse into the Roman finances of the Second Punic War through silver isotopes. *Geochemical Perspect. Lett.* **2**, 127–137.

Albarède F., Desaulty A. M. and Blichert-Toft J. (2012) A geological perspective on the use of Pb isotopes in archaeometry. *Archaeometry* **54**, 853–867.

Argapadmi W., Toth E. R., Fehr M. A., Schönbächler M. and Heinrich C. A. (2018) Silver isotopes as a source and transport tracer for gold: A reconnaissance study at the sheba and new consort gold mines in the barberton greenstone belt, Kaapvaal craton, South Africa. *Econ. Geol.* **113**, 1553–1570.

Baxter D. C., Rodushkin I., Engström E. and Malinovsky D. (2006) Revised exponential model for mass bias correction using an internal standard for isotope abundance ratio measurements by multi-collector inductively coupled plasma mass spectrometry. *J. Anal. At. Spectrom.* **21**, 427.

Beer C., Foldbjerg R., Hayashi Y., Sutherland D. S. and Autrup H. (2012) Toxicity of silver nanoparticles-Nanoparticle or silver ion? *Toxicol. Lett.* **208**, 286–292.

Bendall C., Wigg-Wolf D., Lahaye Y., Von Kaenel H. M. and Brey G. P. (2009) Detecting changes of Celtic gold sources through the application of trace element and Pb isotope laser ablation analysis of Celtic gold coins. *Archaeometry* **51**, 598–625.

Boyle R. W. (1968) *The geochemistry of the silver and its deposits: With Notes on Geochemical Prospecting for the Element*., Geological Survey of Canada, Ottawa.

Brügmann G., Brauns M. and Maas R. (2019) Silver isotope analysis of gold nuggets: An appraisal of instrumental isotope fractionation effects and potential for high-resolution tracing of placer gold. *Chem. Geol.*

Carlson R. W. and Hauri E. H. (2001) Extending the 107Pd- 107Ag chronometer to low Pd/Ag meteorites with multicollector plasma-ionization mass spectrometry. *Geochim. Cosmochim. Acta* **65**, 1839–1848.

Chen J. H. and Wasserburg G. J. (1996) Live 107Pd in the Early Solar System and Implications for Planetary Evolution. In *Earth Processes: Reading the Isotopic Code* (eds. A. Basu and S. Hart). Geophysics Monograph 95. American Geophysical Union. pp. 1–20.

Chugaev A. V. and Chernyshev I. V. (2012) High-Noble Measurement of 107Ag/109Ag in Native Silver and Gold by Multicollector Inductively Coupled Plasma Mass Spectrometry (MC-ICP-MS). *Geochemistry Int.* **50**, 899–910.

Desaulty A.-M., Telouk P., Albalat E. and Albarède F. (2011) Isotopic Ag–Cu–Pb record of silver circulation through 16th–18th century Spain. *Pnas* **108**, 1–6.

Desaulty A. M. and Albarede F. (2013) Copper, lead, and silver isotopes solve a major economic conundrum of Tudor and early Stuart Europe. *Geology* **41**, 135–138.

Fujii T. and Albarede F. (2018) 109Ag–107Ag fractionation in fluids with applications to ore deposits, archeometry, and cosmochemistry. *Geochim. Cosmochim. Acta* **234**, 37–49.

Gough J. and Zilva S. S. (1933) The silver nitrate staining reaction for ascorbic acid in the adrenal, pituitary and ovary of various species of animals. *Biochem. J.* **27**, 1279-1286.1.

Guo Q., Wei H.-Z., Jiang S.-Y., Hohl S., Lin Y.-B., Wang Y.-J. and Li Y.-C. (2017) Matrix Effects Originating from Coexisting Minerals and Accurate Determination of Stable Silver Isotopes in Silver Deposits. *Anal. Chem.* **89**, 13634–13641.

Heslop R. B. and Jones K. (1982) *Anorganická chemie*., Nakladatelství technické literatury, Praha.

Hess D. C. ., Marshall R. R. . and Urey H. C. . (1957) Surface Ionization of Silver; Silver in Meteorites. *Science* **126**, 1291–1293.

Holland G., Tanner S. D., Carlson R. W., Hauri E. H. and Alexander C. M. O. (2001) Matrix-induced isotopic mass fractionation in the ICP-MS. In *Plasma Source Mass Spectrometry:The New Millennium* Royal Society of Chemistry, Cambridge. pp. 288–297.

IAEA (2009) Materials with known 34S/32S isotopic composition. Available at: https://nucleus.iaea.org/rpst/referenceproducts/referencematerials/Stable_Isotopes/34S32S/index.htm [Accessed August 31, 2018].

Irisawa K. and Hirata T. (2006) Tungsten isotopic analysis on six geochemical reference materials using multiple collector-ICP-mass spectrometry coupled with a rhenium-external correction technique. *J. Anal. At. Spectrom.* **21**, 1387–1395.

Johnson C. M., Beard B. L. and Albarede F. (2004) Overview and General Concepts. *Rev. Mineral. Geochemistry* **55**, 1–24.

Junk T., Laycock A. and Renkämper M. (2016) Silver Nanoparticle Tracing Using Stable Isotope Labelling and Multiple Collector ICP-MS (MC-ICP-MS). *Mass Spectrom. Isot. Geochemistry Imp. Coll. London*.

Kaiser T. and Wasserburg G. . J. (1983) The isotopic composition and concentration of Ag in iron meteorites and the origin of exotic silver. *Geochim. Cosmochim. Acta* **47**, 43–58.

Kelly W. R. and Wasserburg G. J. (1978) Evidence for the existence of 107Pd in the early solar system. *Geophys. Res. Lett.* **5**, 1079–1082.

Kramida A., Ralchenko Y., Reader J. and NIST ASD Team (2018) NIST ASD Ionization Energies Data. *NIST At. Spectra Database (ver. 5.6.1)*. Available at: https://physics.nist.gov/cgi-bin/ASD/ie.pl [Accessed April 1, 2019].

Lu D., Liu Q., Zhang T., Cai Y., Yin Y. and Jiang G. (2016) Stable silver isotope fractionation in the natural transformation process of silver nanoparticles. *Nat. Nanotechnol.* **11**, 682–686.

Luo Y., Celo V., Dabek-Zlotorzynska E. and Yang L. (2012) Effects of precipitation and UV photolysis on Ag isotope ratio: experimental studies. *J. Anal. At. Spectrom.* **27**, 299–304.

Luo Y., Dabek-Zlotorzynska E., Celo V., Muir D. C. G. and Yang L. (2010) Accurate and precise determination of silver isotope fractionation in environmental samples by multicollector-ICPMS. *Anal. Chem.* **82**, 3922–3928.

Mathur R., Arribas A., Megaw P., Wilson M., Stroup S., Meyer-Arrivillaga D. and Arribas I. (2018) Fractionation of silver isotopes in native silver explained by redox reactions. *Geochim. Cosmochim. Acta* **224**, 313–326.

Meija J., Coplen T. B., Berglund M., Brand W. A., De Bièvre P., Gröning M., Holden N. E., Irrgeher J., Loss R. D., Walczyk T. and Prohaska T. (2016) Isotopic compositions of the elements 2013 (IUPAC Technical Report). *Pure Appl. Chem.* **88**, 293–306.

Militký J. and Karwowski M. (2013) Gold und Silber bei den Boiern und ihren südöstlichen Nachbarn – numismatische und archäologische Überlieferung. In *Macht des Goldes, Gold der Macht, Forschungen zur Spätantike und Mittelalter 2* (eds. M. Hardt and O. Heinrich-Tamaska). Weinstadt. pp. 17–31.

Murillo-Barroso M., Montero-Ruiz I., Rafel N., Hunt Ortiz M. A. and Armada X. L. (2016) The Macro-Regional Scale of Silver Production in Iberia During the First Millennium BC in the Context of Mediterranean Contacts. *Oxford J. Archaeol.* **35**, 75–100.

Murray S. (2010) Silver Reference Materials - Now there are two. *Alchemist* **24**, 16.

NIST (2015) New NIST Reference Material Provides a Silver Lining for NanoEHS Research | NIST. Available at: https://www.nist.gov/news-events/news/2015/03/new-nist-reference-material-provides-silver-lining-nanoehs-research [Accessed May 20, 2018].

Peiser H. S., Barnes I. L., De Bièvre P., Murphy T. J., Thode H. G., Roth E., de Laeter J. R., Shima M., Holden N. E. and Hagemann R. (1984) Element by element review of their atomic weights. *Pure Appl. Chem.* **56**, 695–768.

Pernicka E. (2014) Possibilities and limitations of provenance studies of ancient silver and gold. In *Metals of power-Early gold and silver (6. Archaeological Conference of Central Germany)* Landesamt für Denkmalpflege und Archäologie Sachsen-Anha, Halle. pp. 153–164.

Powell L. J., Murphy T. J. and Gramlich J. W. (1981) The Absolute Isotopic Abundance and Atomic Weight of a Reference Sample of Silver. *J. Res. Natl. Bur. Stand. (1934).* **87**, 9–19.

Rasberry S. D. (1984) Standard Reference Material 978a. *Natl. Bur. Stand.*, 2.

Rashid M. U., Bhuiyan M. K. H. and Quayum M. E. (2013) Synthesis of silver nano particles (Ag-NPs) and their uses for quantitative analysis of vitamin C tablets. *Dhaka Univ. J. Pharm. Sci.* **12**, 29–33.

Rehkämper M., Schönbächler M. and Stirling C. H. (2001) Multiple collector ICP-MS: Introduction to instrumentation, measurement techniques and analytical capabilities. *Geostand. Newsl.* **25**, 23–40.

Rosman K. J. R. and Taylor P. D. P. (1998) Isotopic compositions of the elements 1997 (Technical Report). *Pure Appl. Chem.* **70**, 217–235.

Schauble E. A. (2004) Applying Stable Isotope Fractionation Theory to New Systems. *Rev. Mineral. Geochemistry* **55**, 65–111.

Schönbächler M., Carlson R. W., Horan M. F., Mock T. D. and Hauri E. H. (2007) High precision Ag isotope measurements in geologic materials by multiple-collector ICPMS: An evaluation of dry versus wet plasma. *Int. J. Mass Spectrom.* **261**, 183–191.

Schönbächler M., Carlson R. W., Horan M. F., Mock T. D. and Hauri E. H. (2008) Silver isotope variations in chondrites: Volatile depletion and the initial 107Pd abundance of the solar system. *Geochim. Cosmochim. Acta* **72**, 5330–5341.

Schuh A., Fritsch A., Ginepro J. Q. Q., Heim M., Shore A. and Thoennessen M. (2010) Discovery of the silver isotopes. *At. Data Nucl. Data Tables* **96**, 531–540.

Schulz A. R., Stanislawiak S., Baumgart S., Grützkau A. and Mei H. E. (2017) Silver nanoparticles for the detection of cell surface antigens in mass cytometry. *Cytom. Part A* **91**, 25–33.

Stathis E. C. (1948) Determination of Silver with Ascorbic Acid. *Anal. Chem.* **20**, 271–271.

Sturgeon R. E., Willie S. N. and Mester Z. (2006) UV/spray chamber for generation of volatile photo-induced products having enhanced sample introduction efficiency. *J. Anal. At. Spectrom.* **21**, 263–265.

Teng F.-Z., Dauphas N. and Watkins J. (2017) Non-Traditional Stable Isotopes: Restrospective and Prospective. *Rev. Mineral. Geochemistry* **82**, 1–26.

Vaněk V. and Velebil D. (2007) Staré hutnictví stříbra. In *Stříbrná Jihlava 2007: studie k dějinám hornictví a důlních prací* Archaia. pp. 188–205.

Walder A. J. and Freedman P. A. (1992) Isotopic ratio measurement using a double focusing magnetic sector mass analyser with an inductively coupled plasma as an ion source. *J. Anal. At. Spectrom.* **7**, 571–575.

Waldhauser J. (2003) Das Silber der Kelten in Böhmen. In *Man and Mining. Studies in honour of Gerd Weisgerber* (eds. T. Stöllner, G. Körlin, G. Steffens, and J. Cierny). Bochum. pp. 503–512.

Wood J. R., Montero-Ruiz I. and Martinón-Torres M. (2019) *From Iberia to the Southern Levant: The Movement of Silver Across the Mediterranean in the Early Iron Age*., Springer US.

Woodland S. J., Rehkämper M., Halliday A. N., Lee D. C., Hattendorf B. and Günther D. (2005) Accurate measurement of silver isotopic compositions in geological materials including low Pd/Ag meteorites. *Geochim. Cosmochim. Acta* **69**, 2153–2163.

Wu S. and Meng S. (2005) Preparation of ultrafine silver powder using ascorbic acid as reducing agent and its application in MLCI. *Mater. Chem. Phys.* **89**, 423–427.

Yang L., Dabek-Zlotorzynska E. and Celo V. (2009) High precision determination of silver isotope ratios in commercial products by MC-ICP-MS. *J. Anal. At. Spectrom.* **24**, 1564–1569.